

Lignin/Puerarin Nanoparticle-Incorporated Hydrogel Improves Angiogenesis through Puerarin-Induced Autophagy Activation

Yingjing Pan^{1,*}, Tianci Lin^{1,*}, Longquan Shao², Yulin Zhang², Qiao Han³, Liyuan Sheng⁴, Rui Guo⁵, Ting Sun¹, Yanli Zhang²

¹Foshan Stomatological Hospital, School of Medicine, Foshan University, Foshan, 528225, People's Republic of China; ²Stomatological Hospital, School of Stomatology, Southern Medical University, Guangzhou, 510280, People's Republic of China; ³Stomatology Hospital of Guangzhou Medical University, Guangzhou, 510182, People's Republic of China; ⁴Shenzhen Institute, Peking University, Shenzhen, 518057, People's Republic of China; ⁵Department of Biomedical Engineering, Jinan University, Guangzhou, 510632, People's Republic of China

*These authors contributed equally to this work

Correspondence: Ting Sun, Foshan Stomatological Hospital, School of Medicine, Foshan University, Foshan, 528225, People's Republic of China, Email sun_ting1985@qq.com; Yanli Zhang, Stomatological Hospital, School of Stomatology, Southern Medical University, Guangzhou, 510280, People's Republic of China, Email 541292702@qq.com

Purpose: Puerarin is the main isoflavone extracted from *Radix Puerariae lobata* (Willd.) and exerts a strong protective effect on endothelial cells. This isoflavone also exerts proven angiogenic effects; however, the potential underlying mechanism has not been fully explored. Here in this work, we aimed to determine the proangiogenesis effect of a puerarin-attached lignin nanoparticle-incorporated hydrogel and explore the underlying mechanism.

Materials and Methods: Puerarin-attached lignin nanoparticles were fabricated and mixed with the GelMA hydrogel. After the hydrogel was characterized, the angiogenic effect was evaluated in a mouse hind-limb ischemia model. To further explore the mechanism of angiogenesis, human endothelial cell line EA.hy926 was exposure to different concentrations of puerarin. Wound healing assays and tube formation assays were used to investigate the effects of puerarin on cell migration and angiogenesis. qPCR and Western blotting were performed to determine the changes in the levels of angiogenesis indicators, autophagy indicators and PPAR β/δ . 3-MA was used to assess the role of autophagy in the puerarin-mediated angiogenesis effect in vivo and in vitro.

Results: The hydrogel significantly improved blood flow restoration in mice with hind-limb ischemia. This effect was mainly due to puerarin-mediated increases in the angiogenic capacity of endothelial cells and the promotion of autophagy activation. A potential underlying mechanism might be that puerarin-mediated activation of autophagy could induce an increase in PPAR β/δ expression.

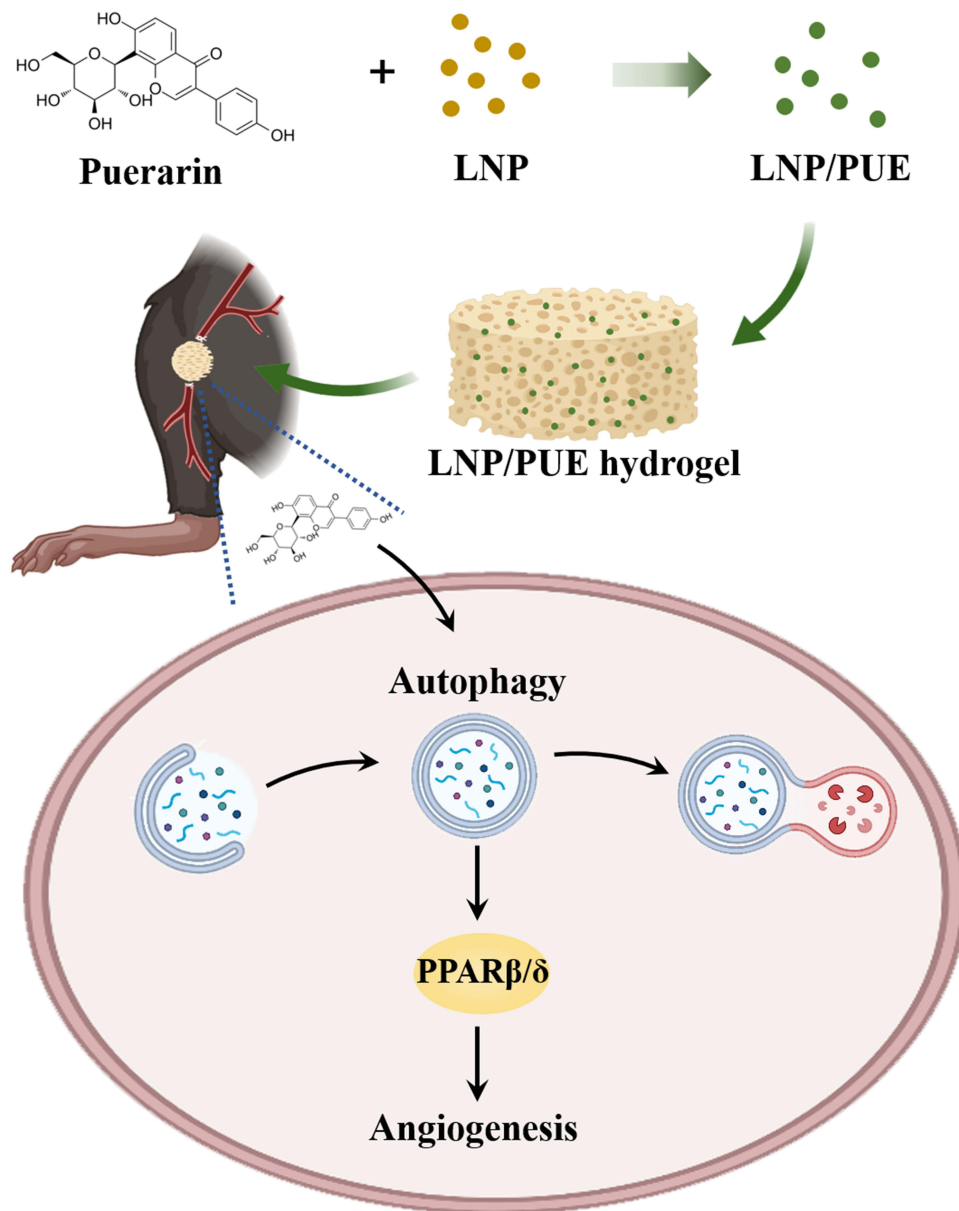
Conclusion: The puerarin-attached lignin nanoparticle-incorporated hydrogel effectively alleviated blood perfusion in mice with hind-limb ischemia. Puerarin has a prominent proangiogenic effect. The potential mechanisms might be that puerarin-mediated autophagy activation and increase in PPAR β/δ .

Keywords: puerarin, angiogenesis, autophagy, PPAR β/δ , vascular endothelial cell

Introduction

As an isoflavone derivative, puerarin (chemical structure of the puerarin molecule shown in Figure 1H) is the main active component extracted from dry root of the traditional Chinese medicine (TCM) *Radix Puerariae lobata* (Willd.). Similar to many TCMs that are thought to exert “activating blood” effects, the beneficial effects of puerarin as shown by TCM theory have been supported by modern medical technology.¹ Puerarin has been shown to promote vasodilation and is considered a clinical treatment for ischemic heart diseases and ischemic cerebrovascular disease.^{2,3} However, endothelial cells (ECs) not only participate in vasoconstriction and vasodilation but also play key roles in vascular formation. Angiogenesis is widely involved in multiple physiological and pathological processes. Improving vessel formation has

Graphical Abstract



been a hot topic in ischemic disease therapy and tissue regeneration research.^{4,5} Studies have shown that puerarin can exert protective effects on ECs under pathological conditions such as inflammation, oxidative stress, and endothelial-mesenchymal transition (EMT).^{6,7} The angiogenic effect of puerarin has been supported by evidence of enhanced levels of angiogenesis factors, such as VEGFA, in rats.⁸ However, the detailed molecular mechanisms by which puerarin induces angiogenesis have not been extensively studied.

Autophagy is a process by which cells self-degrade and recycle intracellular components, and it participates in many cellular processes, including angiogenesis.^{9,10} In many neovascularization diseases, such as tumors, macular degeneration and diabetic retinopathy, the promotion of autophagy can be detected in vessels.^{11–13} In vitro experiments have shown that suppressing of autophagy can evidently inhibit the migration and tube formation abilities of ECs.¹⁴ The reason of this effect might be that the promotion of autophagy can accelerate the degradation and recycling of intracellular

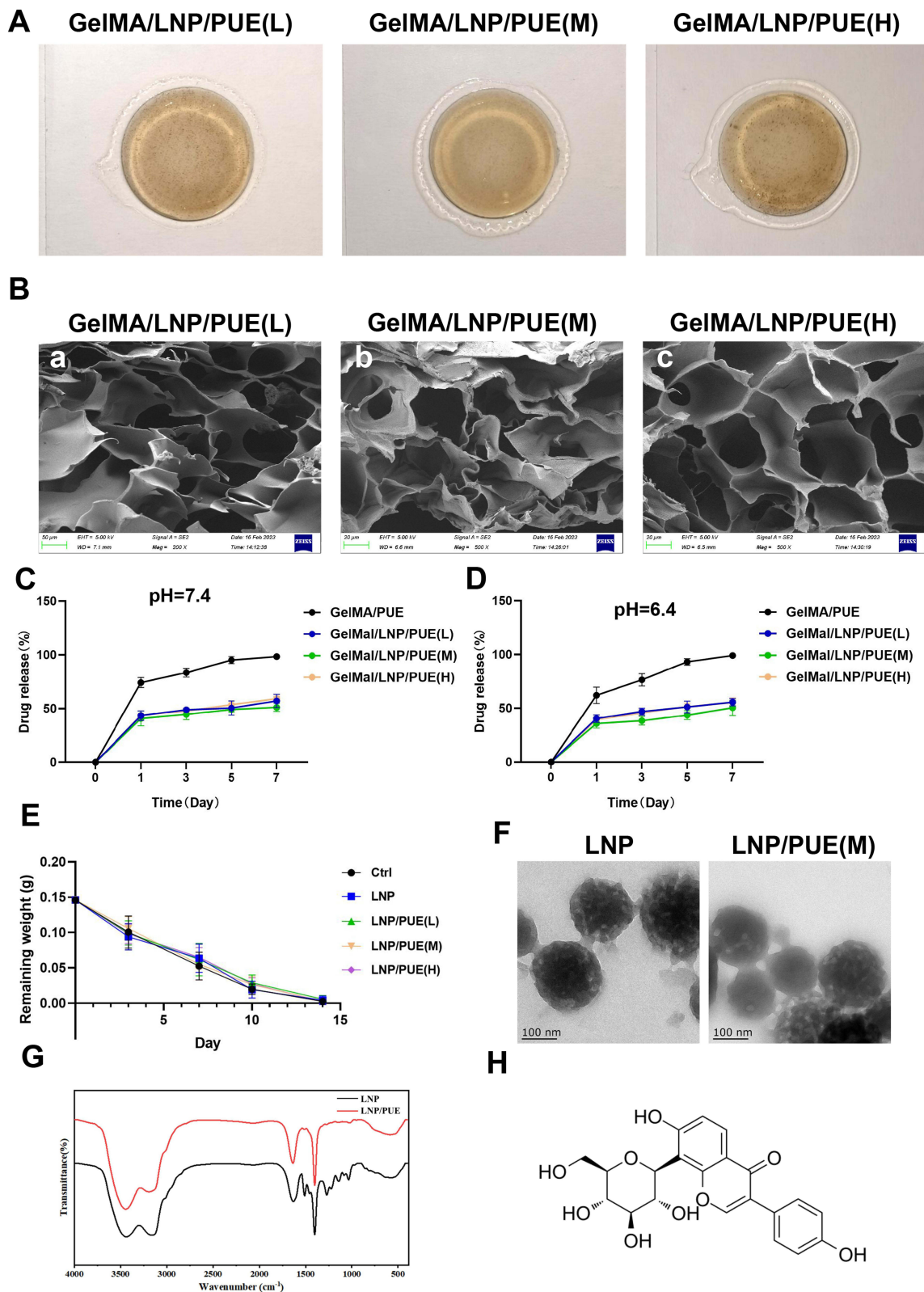


Figure 1 Material characterization. **(A)** Images of LNP/PUE-incorporated hydrogel. **(B)** SEM results of the LNP/PUE-incorporated hydrogels ((a) scale bar=50 µm, (b, c) scale bar=20 µm). **(C)** Drug-release percentages of the hydrogels under pH=7.4. **(D)** Drug-release percentages of the hydrogels under pH=6.4. **(E)** In vivo degradation of LNP/PUE-incorporated hydrogel. **(F)** TEM results of LNP and LNP/PUE. **(G)** FTIR results of LNP and LNP/PUE; **(H)** Chemical structure of the puerarin molecule.

substances to provide more sufficient energy for the angiogenesis process. It has been demonstrated that puerarin can regulate autophagy; for example, this isoflavone can activate autophagy in chondrocytes to alleviate osteoarthritis.¹⁵ Another study suggested that puerarin could promote autophagy in an AMPK-dependent manner and protect ECs against hyperglycemia-induced chronic vascular disease.¹⁶ However, whether this puerarin-mediated autophagy can further induce angiogenesis remains unknown.

Peroxisome proliferator-activated receptor β/δ (PPAR β/δ) belongs to the PPAR family and participates in energy homeostasis and metabolic function.¹⁷ Previous reports have indicated that PPAR β/δ activation can promote fatty acid metabolism.¹⁸ Moreover, this factor may have a close relationship with autophagy. It has been suggested that PPAR β/δ can accelerate bone regeneration by activating the AMPK/mTOR pathway and subsequently promote autophagy levels by inhibiting mTOR.¹⁹ PPAR β/δ can also promote autophagic flux in hepatic cells and contribute to lipid deposition.²⁰ On the other hand, PPAR β/δ plays a nonnegligible role in cell migration and invasion and is considered a proangiogenic factor.²¹ This factor can promote vascular repair by interacting with HIF1 α after ischemia.²² In tumor tissue, PPAR β/δ can promote angiogenesis in an IL-8-related manner both in vivo and in vitro.^{23,24} In our study, puerarin promoted PPAR β/δ elevation. However, whether there is a relationship between puerarin-mediated autophagy and PPAR β/δ -related angiogenesis has not yet been explored.

In this study, we chose lignin nanoparticles (LNPs) as scaffold to attach puerarin. LNPs are novel green nanoparticles that have been used in vivo as efficient candidate for drug and gene delivery.²⁵ We prepared and characterized puerarin-attached LNPs (LNP/PUE) and mixed them with GelMA hydrogel to construct a puerarin sustained-release system. After determining the proangiogenic effect of the composite material in a mouse hind-limb model, the underlying molecular mechanism was further explored. The treatment of EA.hy926 cells with puerarin induced migration and tube formation were observed. Autophagy activation and overexpression of the ligand-activated transcription factor PPAR β/δ were also examined. Autophagy inhibitor could significantly suppress this puerarin-induced autophagy and PPAR β/δ activation and angiogenesis in both in vivo and in vitro studies. Therefore, we hypothesized that puerarin could mediate angiogenesis through autophagy-induced PPAR β/δ upregulation. Our findings may provide theoretical evidence for the development of biomedical applications of puerarin to mediate angiogenesis.

Materials and Methods

Preparation and Characterization of the LNP/PUE-Incorporated Hydrogel

LNP/PUE were produced using antisolvent precipitation according to the method described by Ou et al.²⁶ A total of 60 mg of alkaline lignin (Sigma, 370959) was dissolved in 10 mL of methanol and stirred using a magnetic stirring apparatus for 2 h. The insoluble sediment was removed after brief centrifugation at 800 rpm. Then, lignin solution was stirred by a magnetic stirring apparatus, and distilled water was added. For every 2 mL lignin solution, 6 mL distilled water was added. After all the water was added, stirring was continued for 10 min and then the sample was centrifuged at 10,000 \times g for 10 min. The sediment was collected, stored at -80°C overnight and dried by freeze-vacuuming (CoolSafe1104, LaboGene) for 24 h to obtain LNP powder. 10 mg of LNPs were resuspended in 100 μL of PBS. Different concentrations of puerarin (PUE(L)=2.5 mM, PUE(M)=5 mM, PUE(H)=25 mM) were mixed and incubated with the LNP suspension. Then, the mixture was mixed thoroughly and stored at -80°C overnight before being frozen under vacuum to obtain LNP/PUE. FTIR of LNP/PUE was performed with a BRUKER TENSOR 27 to evaluate the functional groups and chemical bonds of the LNPs and puerarin. The morphological structures of LNP and LNP/PUE was determined by TEM (HITACHI, H-7500).

The GelMA hydrogel was purchased from EFL (EFL, EFL-GM-30) and prepared according to the manufacturer's instructions. LNP/PUE nanoparticles were mixed with GelMA at a concentration of 2.5 mg/mL. The gel was injected into a circular mold with an inner diameter of 1 cm and was cured using an UV lamp to obtain LNP/PUE-incorporated hydrogel. The surface morphology of the hydrogel was observed by SEM (JSM, IT300). Sustained release of puerarin was detected by HPLC. The hydrogels in each group were subcutaneously put into mice after weighed. The weight of each hydrogel was recorded on days 3, 7, 10 and 14 to evaluate the in vivo degradation.

Mouse Hind Limb Ischemia Model Construction

Animal experiment were strictly followed by Laboratory animals—General code of animal welfare (OIE Terrestrial animal health code—Chapter 7.8—Use of animals in research and education, MOD). Male C57BL/6 mice weighing 22 ± 2 g were purchased from the Laboratory Animal Center of Southern Medical University. The experiments were approved by the Animal Ethics Committee of Guand Dong Hua Wei Testing Co, Ltd (Grant No.202207003) and were performed in strict accordance with the guidelines pertaining to experimental animal care and use in China. Unilateral femoral artery ligation was performed as described by Padgett et al.²⁷ Briefly, after the mice were anesthetized, the right femoral artery was exposed. The proximal femoral artery and distal saphenous artery were ligated, and an arterectomy was performed. GelMA, GelMA/LNP, GelMA/LNP/PUE(L), GelMA/LNP/PUE(M), and GelMA/LNP/PUE(H) were placed at the dissection areas in the control, LNP/PUE, LNP/PUE(L), LNP/PUE(M) and LNP/PUE(H) groups (n=6 for each group), respectively. In the LNP/PUE + 3-MA groups, 15 μ L of 5 mg/mL 3-methyladenine (3-MA) (MCE, HY-19312) was added to the hydrogel. Perfusion conditions were examined immediately after the operation and on day 7 and 14 after the operation using a laser speckle contrast imaging imager (RWD, RFLSI ZW/RFLSI III). 14 days after the operation, gastrocnemius tissues were collected from the mice for further analysis.

Tissue Staining

Mouse gastrocnemius tissue was harvested and fixed in 4% formaldehyde. The tissue was then sliced after being dehydrated and paraffin-embedded. After being dewaxed, the sections were quenched with 3% hydrogen peroxide and boiled with 0.01 M citric acid buffer (pH 6.0). Then, after being incubated with CD31 antibody (28083-1-AP, Proteintech, China) at 4°C overnight and being washed, the slices were then treated with secondary antibodies. The slices were backstained with hematoxylin and images were taken with an Olympus BX63 microscope.

Cell Culture

The human EC line EA.hy926 was provided by the Chinese Academy of Science Cell Bank (Shanghai, China). The cells were cultured in Dulbecco's modified eagle's medium (DMEM, C11995500BT, Gibco, US) containing 10% fetal bovine serum (FBS) (164210-50, Procell, China) in a humidified 37°C incubator with 5% CO₂. Passaging was performed when the cells grew to 80% to 90% confluence. EA.hy926 cells were incubated with 10, 25, and 50 μ M puerarin with or without 10 mM 3-MA, an autophagy inhibitor. Two hours before the treatment, 3-MA was pre added to the culture medium.

Cell Proliferation and Viability Assays

Cell viability was assessed by MTT assays as described by Zhou et al.²⁸ EA.hy926 cells (2×10^3 per well) were inoculated into a 96-well plate allowed to adhere for 24 h, and then exposed to 5, 10, 25, 50 or 100 μ M puerarin (HY-N0145, MCE, US) for 6, 24 and 48 h, and each group included 6 replicates. Then, 5 mg/mL MTT was added to each well and the plate was incubated for another 4 h. Then, 150 μ L of DMSO was added into each well, and the samples were oscillated on a shaker for 10 min. The absorbance at 490 nm was recorded.

Cell Migration Assays

The migration ability of EA.hy926 cells was detected by wound healing assays as described in our previous study.²⁹ Cells were inoculated onto 12-well plates and cultured until the density reached 100%. Scratches on the cell monolayer were made with a 200 μ L micropipette tip. Puerarin was diluted to 10, 25 and 50 μ M in DMEM without FBS, and added into the plate and incubated for 24 h. As described by Mishra et al.³⁰ cells in the 3-MA and 3-MA + puerarin groups were exposed to 10 mM 3-MA for 2 h before the drug was added. Then, the supernatant was discarded and replaced with culture medium with or without a certain concentration of puerarin. Photographs were taken after 0, 12 and 24 h of treatment. ImageJ software was used to measure the recovery area in each group.

Tube Formation Assays

Tube formation ability of puerarin-treated EA.hy926 was assessed as previously described.²⁹ The cells were pretreated by puerarin for 12 h. Similar to the migration assays, the cells in the 3-MA and 3-MA + puerarin groups were treated with 3-MA in culture medium for 2 h before being treated with puerarin. Then, 100 μ L of Matrigel (356237, BD, US) was added to a 96-well plate and placed in an incubator for 30 min until it solidified. The pretreated cells were then resuspended in FBS-free medium and inoculated in the Matrigel-coated plates at a density of 2×10^4 cells per well. Photographs were taken at 6, 12 and 24 h. Tubular structures were defined using ImageJ and the Angiogenesis Analysis plugin.³¹

Quantitative Real-Time Polymerase Chain Reaction (qPCR)

RNA was obtained from puerarin-treated EA.hy926 cells using a Total RNA Isolation Kit (RC112-01, Vazyme, China) and reverse transcribed into cDNA using All-in-one RT SuperMix (R333-01, Vazyme, China) for qPCR. SYBR Green Master Mix (AG11701, Accurate Biology, China) and a LightCycler 480 (Roche, Swiss) were used to perform qPCR. The OD results were normalized against GAPDH expression. The primers in this work are listed in Table 1.

Western Blotting (WB)

For animal samples, gastrocnemius tissues were harvested and immediately placed into liquid nitrogen. The frozen samples were then placed into RIPA lysis buffer (BB-32012, Bestbio, China) and homogenized. For in vitro experiments, EA.hy926 cells were exposed to 10, 25 and 50 μ M puerarin for 0, 1, 3, 6, 12 and 24 h. Total protein was extracted from tissue and cell samples with RIPA lysis buffer according to the instructions. The sample concentrations were assessed by a BCA kit (23223, Thermo Fisher, US) and normalized. The extracts were then separated by SDS-PAGE and transferred onto PVDF membranes (IPVH00010, Millipore, US). The membranes were then treated with Quickblot buffer (P0252, Biotime, China). Primary antibodies and secondary antibodies were used to sequentially treat the membranes. The gray values were evaluated by ImageJ software.

Immunofluorescence

2×10^4 of EA.hy926 cells were inoculated onto each cell slides in a 24-well plate and treated with puerarin with or without 3-MA for 12 h. The slides were then fixed with 4% paraformaldehyde. After 10 min of treatment with 0.1% Triton X-100 (P0096, Biotime, China) and being blocked with 5% BSA (SW3015, Solarbio, China) for 1 h at 37°C, the cells were incubated with LC3 antibodies (ab48394, Abcam, UK) overnight. Then the cells were incubated with the secondary antibody (ZF-0511, ZSGBbio, China) for 1 h. DAPI (C0065, Solarbio, China) was then used to stain the cell nuclei. And the fluorescence intensity was observed with an Olympus BX63 microscope.

Statistical Analysis

All the results in this manuscript are presented as the means \pm standard deviations. Significant differences between groups were evaluated by one-way ANOVA or two-tailed Student's *t*-test using SPSS version 20.0. Experiments were repeated at least three times. The significance is displayed in the figures as *($P < 0.05$), **($P < 0.01$) and ***($P < 0.001$) or #($P < 0.05$), ##($P < 0.01$) and ###($P < 0.001$).

Table 1 The Primer Sequences Used for qPCR

Gene	Forward Primer Sequence (5'-3')	Reverse Primer Sequence (5'-3')
VEGFA	CTTCTGGGCTGTTCTCGCTTCG	CTCCTCTTCCTTCTCTTCTTCCTCCTC
VEGFR2	CTGGCTACTTCTTGTCATCATCCTACG	TGGCATCATAAGGCAGTCGTTACAC
ANGI	CGCTGCCATTCTGACTCACATAGG	CGTACTCTCACGACAGTTGCCATC
ANGII	CAGAACCAGACGGCTGTGATGATAG	AGTGTTCCAAGAGCTGAAGTTCAAGTC
Tie2	TGCTTGGACCCCTAGTGACATTCTTC	TCTTGCCTTGAACCTTGTAACGGATAG
GAPDH	AATGGGCAGCCGTTAGGAAA	GCGCCCAATACGACCAAAATC

Results

Characterization of the LNP/PUE Hydrogel

The LNP/PUE hydrogel was prepared (Figure 1A) and characterized. The LNP/PUE FTIR results suggested that there were no chemical bonds between puerarin and LNP (Figure 1G). The TEM results indicated that both LNP and LNP/PUE showed spherical structures and the addition of PUE did not significantly affect LNPs morphology (Figure 1F). The SEM results showed that the hydrogel had a porous structure (Figure 1B). PUE release behavior was determined by HPLC under pH=7.4 (Figure 1C) and pH=6.4 (Figure 1D). The puerarin release rate in the GelMA/PUE groups was markedly faster than that in the GelMA/LNP/PUE groups, which indicated that the LNPs played an effective role in sustained controlled release as a scaffold for PUE. The results of the in vivo degradation indicated that the degradation rate of the nanomaterials was close to 100% at day 14 after the operation (Figure 1E).

The LNP/PUE Hydrogel Alleviates Blood Flow in Hind-Limb Ischemia Mice

Representative blood flow images are presented in Figure 2A and B, 7 days after the surgery, the blood reperfusion ratios in the LNP/PUE(M) and LNP/PUE(H) groups were evidently higher than those in the control groups ($P<0.001$). On day 14, all three puerarin-treated groups had better blood flow conditions than the control groups ($P<0.001$). Immunohistochemical staining of the gastrocnemius ligation side indicated that there was higher CD31 expression in the medium concentration group ($P<0.001$) and high concentration groups ($P<0.05$) (Figure 2C and D). There were no differences between the control and LNP groups. Muscle tissue protein was then extracted and examined by WB. The results suggested that the proangiogenic indicator VEGFA was prominently increased in the three puerarin groups, and the vessel endothelial biomarker CD31 also showed higher expression levels in the LNP/PUE(M) group than in the LNP and control groups (Figure 3A and B). In the LNP/PUE(H) groups, CD31 was upregulated compared with that in the control groups. There was still no significant difference between the control and LNP groups. These above results suggested that the LNP/PUE hydrogel could alleviate blood flow in hind-limb ischemia mice, especially in the medium concentration groups, and the therapeutic effect was mostly due to the presence of puerarin rather than LNPs. In the following experiment, we aimed to further explain the potential underlying mechanism of the proangiogenic effect of puerarin.

Effect of Puerarin on Cell Viability

We used the human umbilical vein EC line EA.hy926 to examine the potential mechanism of puerarin-induced angiogenesis. First, to determine the appropriate working concentration of puerarin in vitro, MTT assays were performed. As shown in Figure 4A, exposure of EA.hy926 cells to 10, 25, 50 and 100 μM puerarin for 6 h showed slightly enhanced viability. Exposure to 5–50 μM puerarin for 24 h promoted cell proliferation, and exposure to 10, 25 and 50 μM puerarin for 48 h enhanced proliferation. However, the viability of 100 μM puerarin-treated cells was significantly reduced at both 24 and 48 h. These results suggested that 10, 25 and 50 μM puerarin could promote cell viability, whereas 100 μM puerarin was cytotoxic toward EA.hy926 cells. Based on the MTT results, 10, 25 and 50 μM puerarin were chosen for the following experiments.

Puerarin Promotes the Migration of EA.hy926 Cells

A wound healing assay was performed to determine whether puerarin could affect EA.hy926 cell migration (Figure 4B and C). Twelve hours after the scratched were made, the recovery areas in the groups treated with 10, 25 and 50 μM puerarin groups were larger than those in the control group. However, no difference was observed among the puerarin-treated groups. At 24 h, the recovery areas in the 10, 25 and 50 μM groups were larger than those in the control group. Moreover, 50 μM puerarin more effectively promoted cell migration than 10 μM puerarin ($P<0.05$). These results demonstrated that puerarin could promote the migration of EA.hy926 cells and that 50 μM puerarin exerted superior effects compared to 10 μM puerarin.

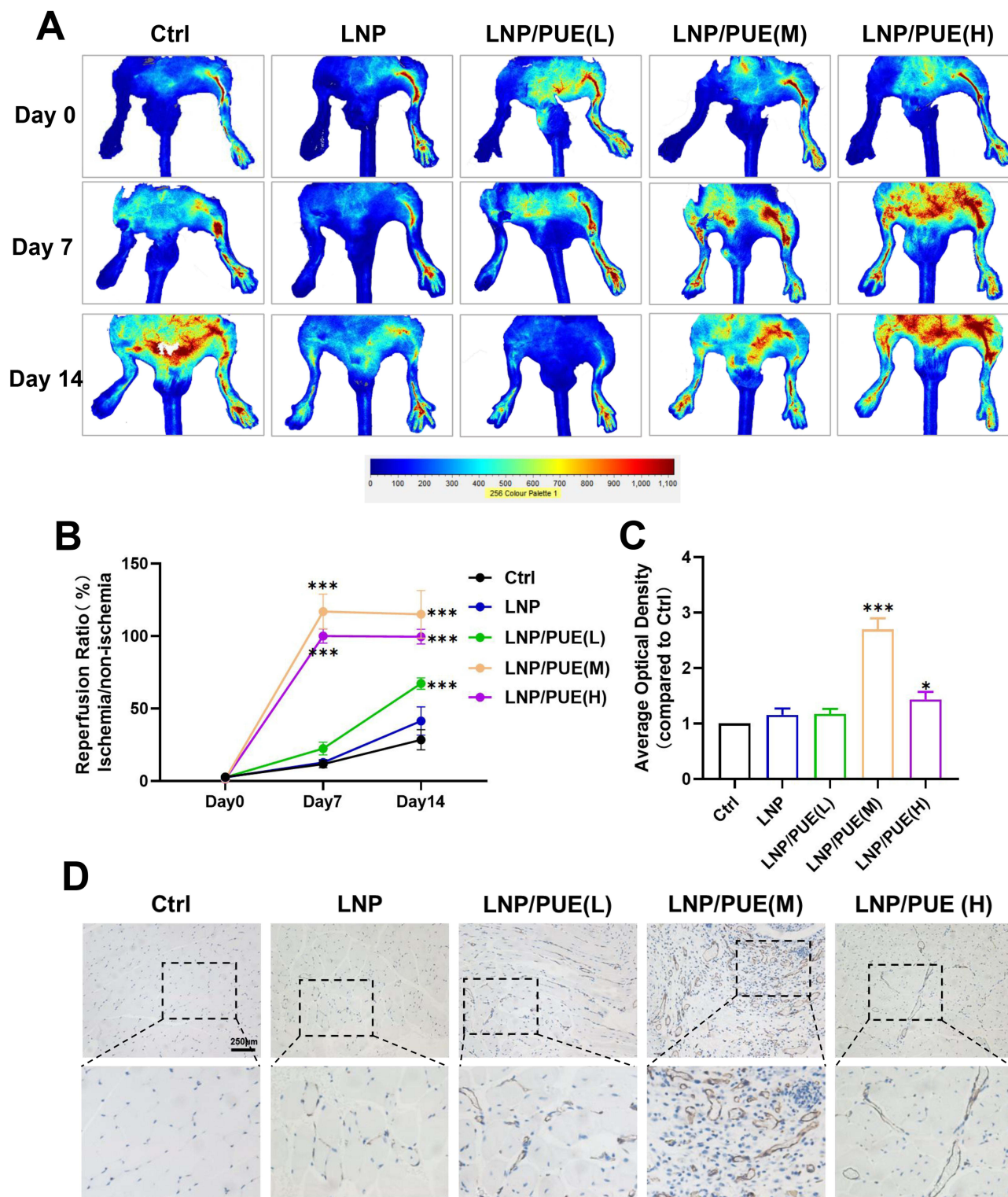


Figure 2 The LNP/PUE-incorporated hydrogel promotes angiogenesis in a mouse hind-limb ischemia model. **(A)** Representative image of blood flow perfusion image of hind-limb ischemia mice on days 0, 7 and 14 after the operation. **(B)** Statistical analysis of **(A)**; **(C)** and **(D)** CD31 immunohistochemical and statistical analysis of mouse gastrocnemius samples on day 14 after the operation (scale bar=250 μm). *($P < 0.05$), ***($P < 0.001$).

Puerarin Promotes Angiogenesis in EA.hy926 Cells

After confirming that puerarin could promote EA.hy926 cell migration, we further determined its effect on angiogenesis via tube formation assays (Figure 4D). As shown in Figure 4E the master segment lengths in the 25 and 50 μM groups

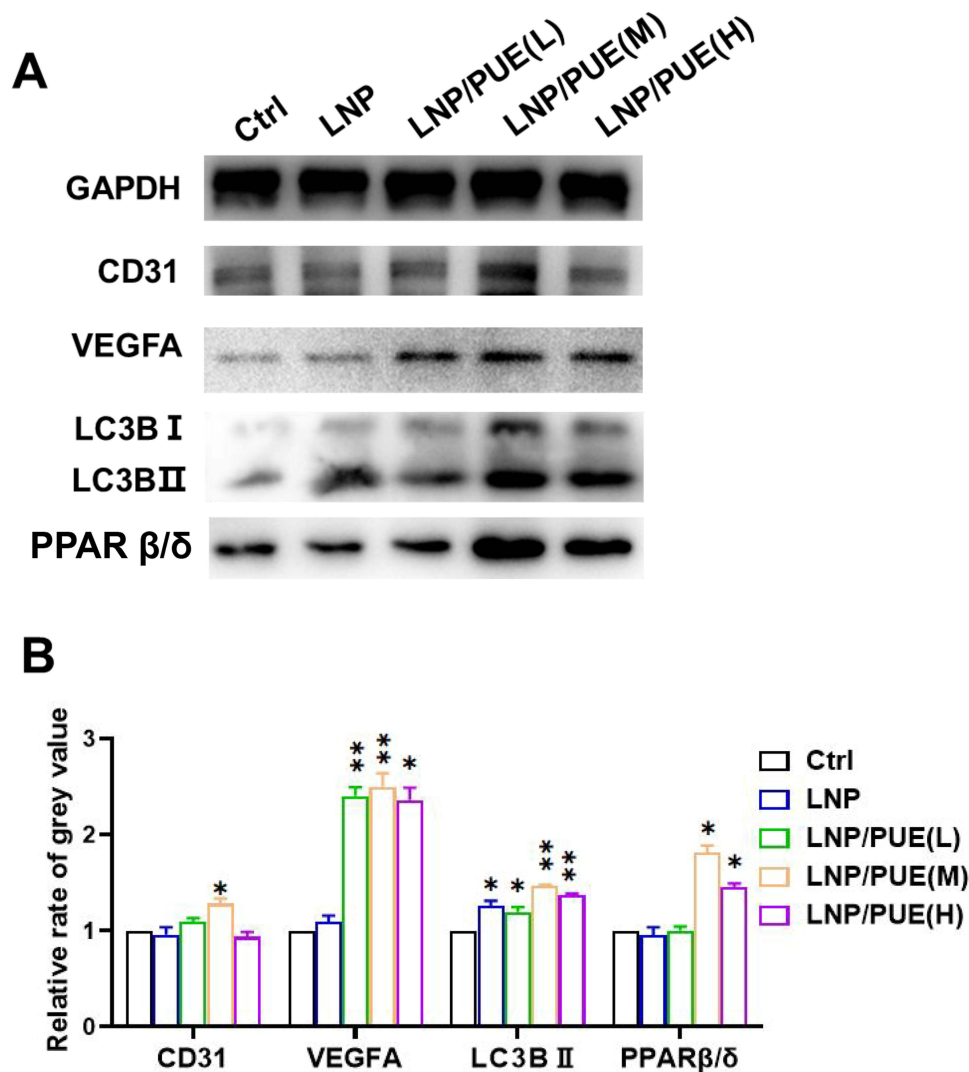


Figure 3 The LNP/PUE-incorporated hydrogel promotes angiogenesis, autophagy and PPAR β/δ elevation in the gastrocnemius tissue of hind-limb ischemic mice. **(A and B)** WB results and the statistical analysis of the tissue samples. * $(P < 0.05)$, ** $(P < 0.01)$.

were enhanced compared with those in the control group. The meshes area and node numbers in the experimental groups were all significantly increased. Among three puerarin-treated groups, the meshes areas and node numbers in the 50 μM group were higher than those of the 10 μM group. Puerarin robustly promoted tube formation in EA.hy926 cells.

Puerarin Promotes Angiogenesis-Related Factor Expression in EA.hy926 Cells

The levels of the angiogenesis-related factors VEGFA, VEGFR2, ANG1, ANG2 and Tie2 were measured by qPCR. Treatment with puerarin (10 μM) for 1, 3, and 6 h increased VEGFA expression, and the mRNA level of VEGFR2 was also increased at 3 h (Figure 5A). VEGFA expression was elevated in the 25 μM puerarin-treated group at all timepoints, and an increase in VEGFR2 upregulation was observed at 3, 6 and 12 h (Figure 5B). Puerarin at a concentration of 50 μM induced a greater increase in VEGFA expression than 10 or 25 μM , and the change in VEGFR2 expression lasted until 24 h (Figure 5C). However, no difference was observed in the expression of ANG1, ANG2 or Tie2.

We further confirmed the changes in VEGFA and VEGFR2 expression at the protein level by WB. Treatment with 10, 25 and 50 μM puerarin for 3 h promoted VEGFA expression, and the effect lasted for 24 h. As shown in Figure 6A, VEGFR2 expression was increased by treatment with 10 μM puerarin for 6, 12 and 24 h. In the 25 and 50 μM puerarin-

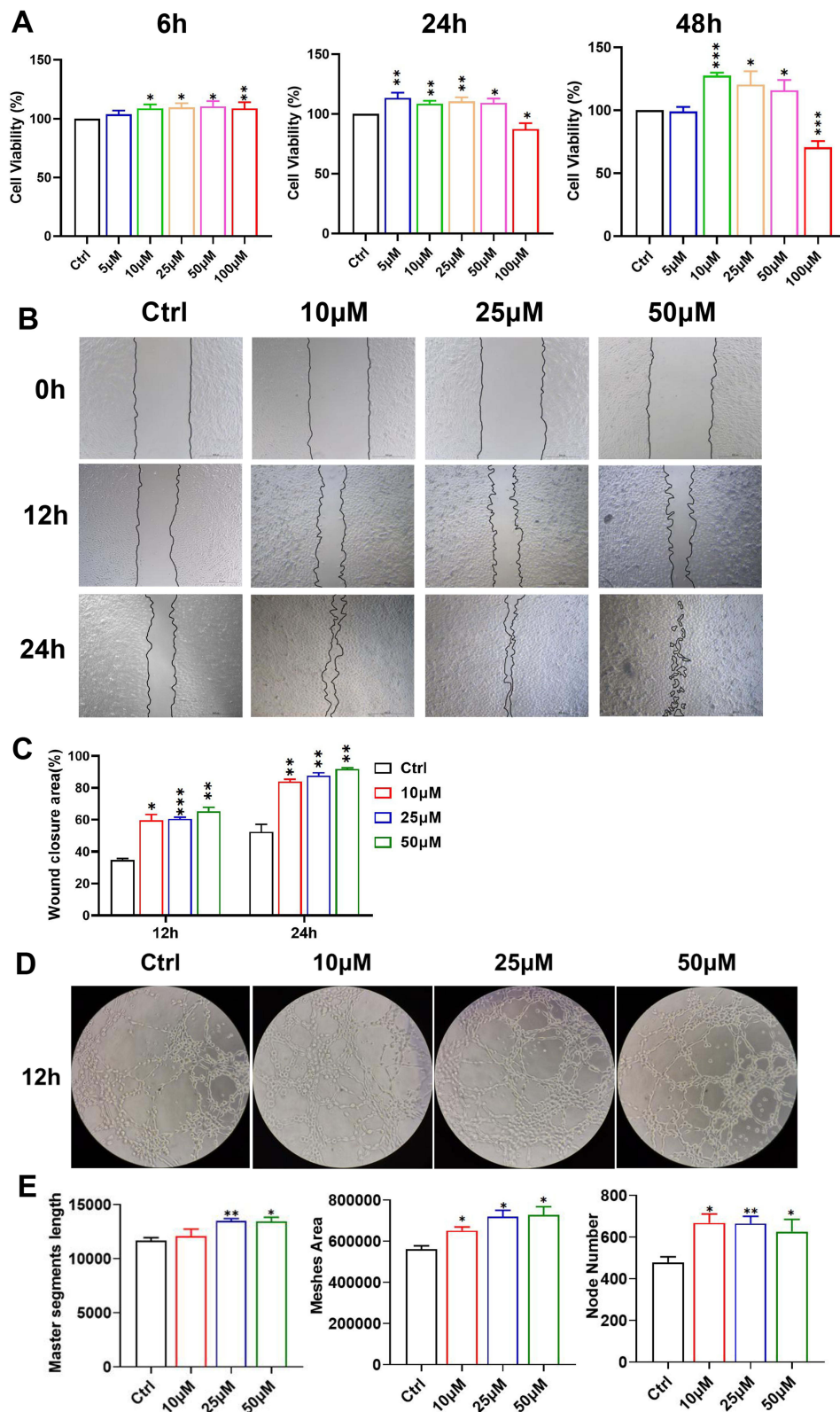


Figure 4 Effects of puerarin on the proliferation, migration and tube formation abilities of EA.hy926 cells. **(A)** The viability of EA.hy926 cells after exposure to puerarin (5, 10, 25, 50 and 100 μ M) for 6, 24 and 48 h; **(B and C)** After exposure to 10, 25 and 50 μ M puerarin for 12 and 24 h, wound healing assays were performed to examine the migration ability of the cells (scale bar=500 μ m). **(D)** After 12 h of exposure to puerarin, the angiogenesis ability of cells was detected (magnification: 100 \times). **(E)** Master segment length, meshes area and node numbers were evaluated in each group. * $(P < 0.05)$, ** $(P < 0.01)$, *** $(P < 0.001)$.

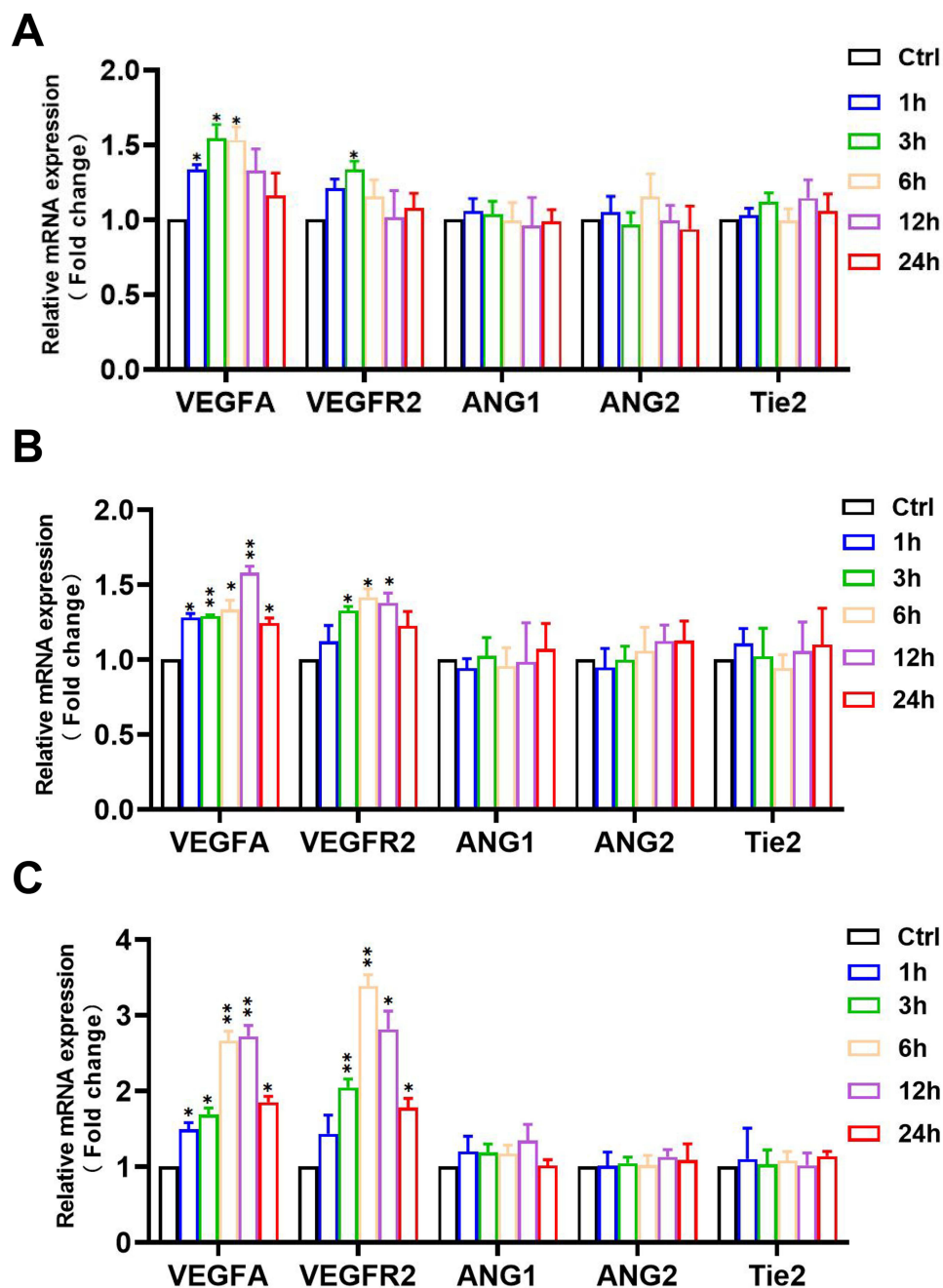


Figure 5 Effects of puerarin on the mRNA expression levels of angiogenesis indicators. After treatment with 10 μM (A), 25 μM (B) and 50 μM (C) puerarin for 1, 3, 6, 12 and 24 h, the mRNA expression levels of VEGFA, VEGFR2, ANG1, ANG2 and Tie2 were determined by qPCR. *($P < 0.05$), **($P < 0.01$).

treated groups, the increase in VEGFR2 expression occurred earlier at 3 h (Figure 6B and C). These results indicated that puerarin could increase the expression of the angiogenesis indicators VEGFA and VEGFR2.

Puerarin Activates Autophagy

The autophagy indicators p62 and LC3BII were examined by WB. As shown in Figure 7A, 10 μM puerarin induced a significant p62 downregulation at 3 h, and the activation of autophagy lasted for 24 h. LC3BII elevated in 12 and 24 h. This promotion was observed in the 25 and 50 μM puerarin-treated groups after 1 h of treatment (Figure 7B and C). Moreover, in the 50 μM puerarin-treated groups, p62 expression was enhanced at 1 and 3 h and then decreased to the control level at 12 and 24 h. This up-then-down trend might be due to the excessive generation of autophagosomes,

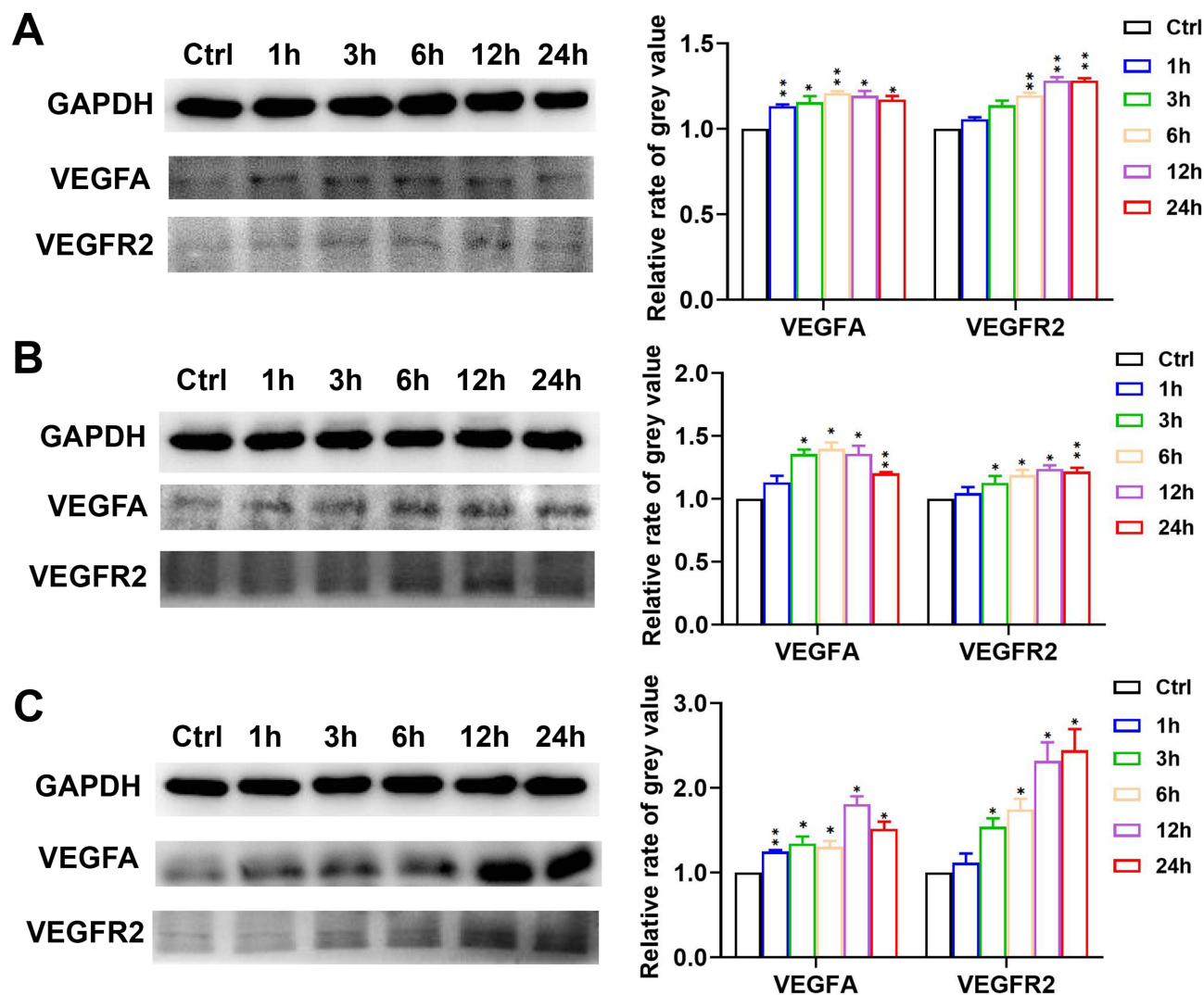


Figure 6 Puerarin promotes the protein expression of VEGFA and VEGFR2. After exposure to 10 μM (A), 25 μM (B) and 50 μM (C) puerarin for 1, 3, 6, 12 and 24 h, the changes in the levels of VEGFA and VEGFR2 were detected by WB. * ($P < 0.05$), ** ($P < 0.01$).

which are generated to such a level that they cannot be rapidly degraded in time during the early stage.³² Immunofluorescence was performed to observe the changes in the LC3BII levels in puerarin-treated cells. Treatment with 50 μM puerarin for 12 h upregulated LC3BII expression in EA.hy926 cells (Figure 7D and E). These indicated that puerarin could activate autophagy in EA.hy926 cells. Similar results were confirmed by WB in animal tissue samples. Compared to those in the control groups, the LC3BII levels in all the puerarin groups were increased (Figure 3A and B). These results indicated that puerarin could activate autophagy both in vivo and in vitro.

Puerarin Induces Angiogenesis via Autophagy-Induced PPAR β/δ Expression

We further examined the levels of the angiogenic factor PPAR β/δ by WB (Figure 8). The results indicated that 10 μM and 25 μM puerarin for 1, 3, 6 and 12 h promoted PPAR β/δ expression. In the 50 μM puerarin-treated groups, the enhancement of PPAR β/δ expression lasted for 24 h. Puerarin induced significant PPAR β/δ overexpression in EA.hy926 cells. Consistently, a significant increase in PPAR β/δ was observed in animal tissue in the medium- and high-concentration groups (Figure 3A and B).

To investigate the relationship between puerarin-induced autophagy activation and PPAR β/δ -mediated angiogenesis, we used an autophagy inhibitor 3-MA and observed its effect on PPAR β/δ expression and angiogenesis (Figure 9A and B).

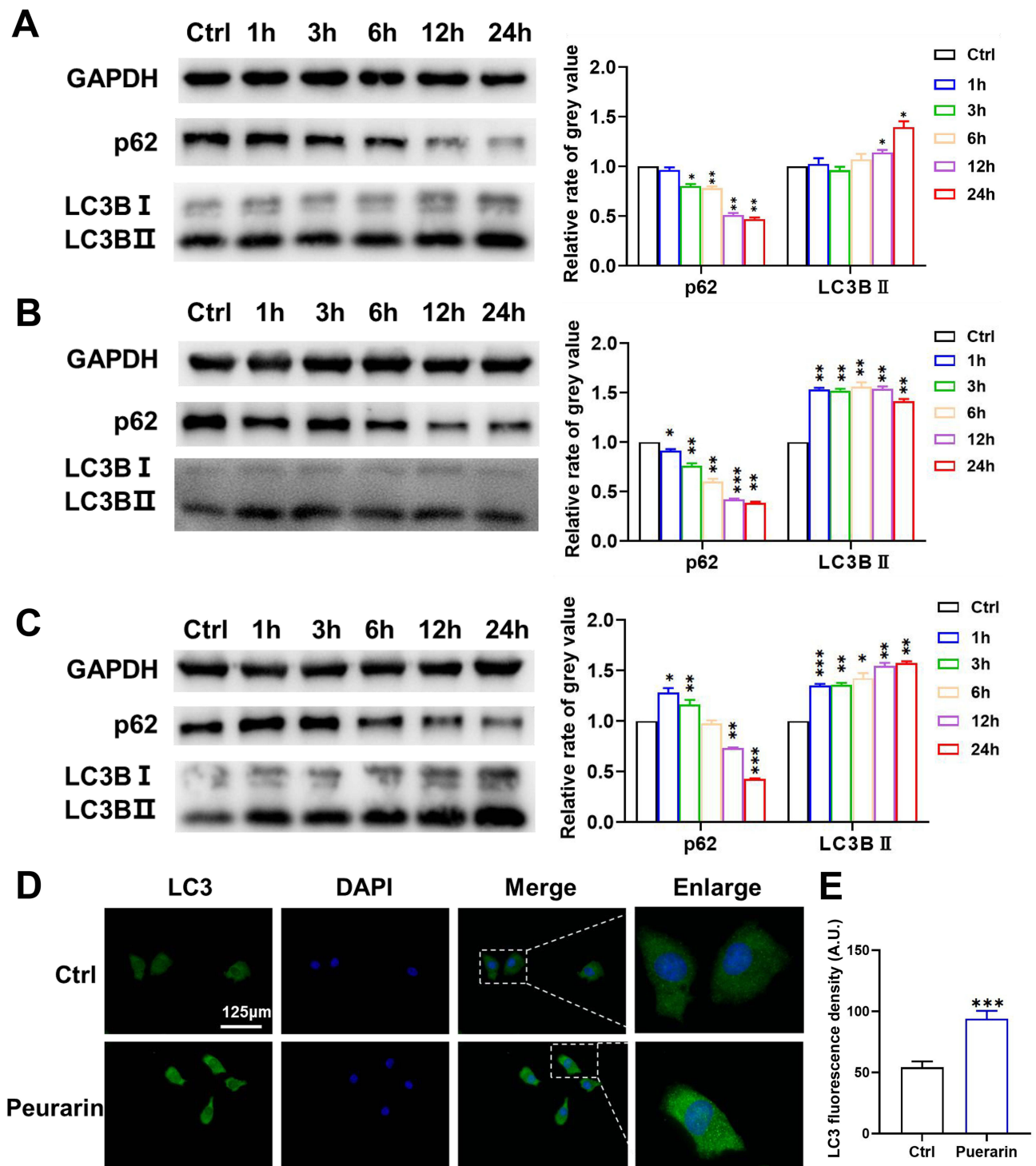


Figure 7 Puerarin activates autophagy in EA.hy926 cells. The expression levels of LC3B and p62 in the 10 μ M (A), 25 μ M (B) and 50 μ M (C) puerarin-treated groups at each timepoint were detected by WB. (D) After treatment with 50 μ M puerarin, the level of LC3B was observed by immunofluorescence analysis (scale bar=125 μ m). (E) Statistical analysis of the data in (D). *($P < 0.05$), **($P < 0.01$), ***($P < 0.001$).

The Western blot results showed that 3-MA successfully suppressed autophagy and PPAR β/δ expression, which suggested that autophagy could regulate PPAR β/δ expression. Furthermore, the expression of the angiogenesis indicators VEGFA and VEGFR2 was significantly decreased, which suggested that the angiogenic effect was inhibited by 3-MA. The 3-MA + puerarin group exhibited increased LC3BII expression and significantly lower p62 levels than the 3-MA group, suggesting

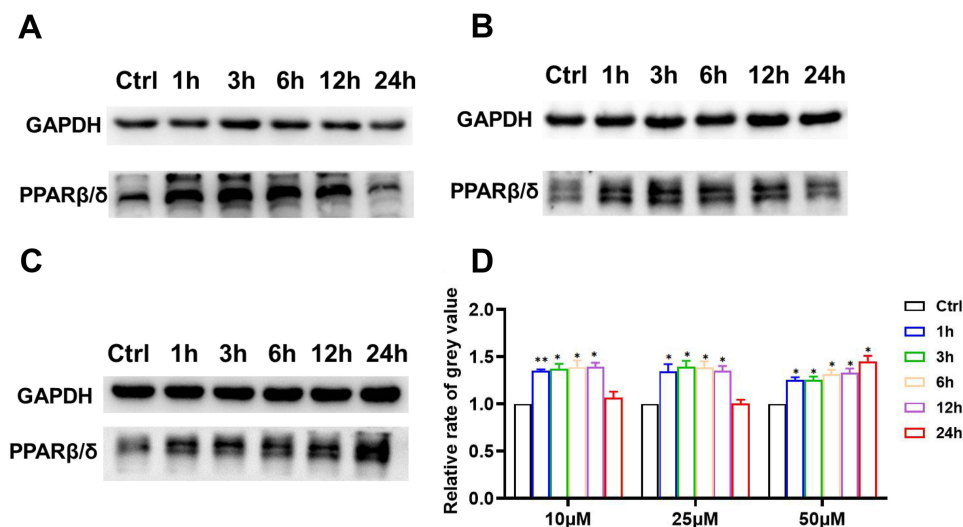
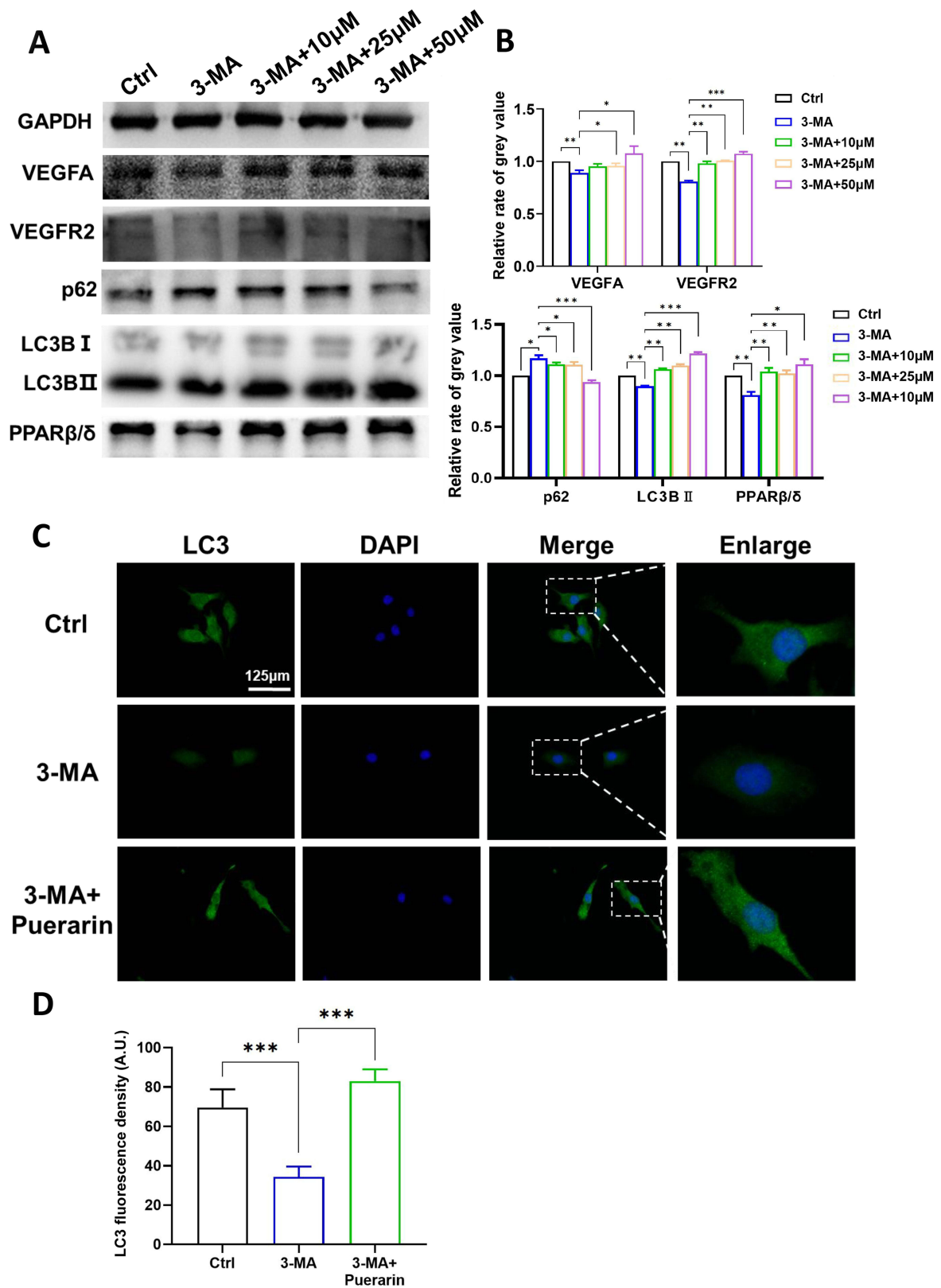


Figure 8 Puerarin increases PPARβ/δ levels. After exposure to 10 μM (A), 25 μM (B) and 50 μM (C) puerarin, the level of PPARβ/δ was detected by WB. (D) Statistical analysis of (A–C). *($P < 0.05$), **($P < 0.01$).

that puerarin abrogated 3-MA-mediated suppression of autophagy. Similar results were observed by immunofluorescence analysis (Figure 9C and D). The fluorescence intensity of GFP-labeled LC3 in the 3-MA + 50 μM puerarin group was brighter than that in the 3-MA group. Moreover, the changes in the expression of VEGFR2, VEGFA and PPARβ/δ were alleviated by puerarin, which suggested that puerarin could suppress angiogenesis by inhibiting autophagy. We further demonstrated that 3-MA exerted an antiangiogenic effect through migration and tube formation assays, and similar results were obtained. As shown in Figure 10A and B, after 24 h, the wound recovery areas in the 3-MA-treated groups ($14.65 \pm 0.17\%$) were prominently smaller than those in the control group ($37.80 \pm 0.71\%$). Moreover, the wound recovery areas in the 10, 25 and 50 μM puerarin groups reached $22.84 \pm 0.83\%$, $31.36 \pm 1.15\%$ and $46.77 \pm 0.25\%$, respectively, which suggested that puerarin treatment alleviated the decrease in migration. Similarly, in tube formation assays (Figure 10C), the master segment length (Figure 10D), meshes area (Figure 10E) and node numbers (Figure 10F) were all decreased after autophagy inhibition and were significantly restored in the 3-MA + puerarin groups. Furthermore, the 3-MA + 50 μM puerarin groups showed an even longer segment length and larger junction number than the control group. The autophagy inhibitor 3-MA was also used on a mouse hind-limb ischemia model to verify our hypothesis. LNP/PUE(M) was chosen for this rescue assay because it exerted the most significant proangiogenic effect. As shown in Figure 11A and D, the blood reperfusion ratio in the LNP/PUE+3-MA group was evidently lower than that of the LNP/PUE groups. WB results also indicated that 3-MA significantly weakened puerarin-induced autophagy and PPARβ/δ expression, and the levels of the angiogenesis indicators VEGFA and CD31 were also decreased (Fig. 11B). 3-MA suppressed CD31 decrease, as observed by immunohistochemistry (Figure 11C and E). The above results suggested that puerarin could promote angiogenesis via autophagy-induced PPARβ/δ enhancement.

Discussion

Angiogenesis refers to the process by which new blood vessels grow from existing capillaries and retro capillary venules.³³ Due to its involvement in a variety of physiological processes, particularly tissue repair, angiogenesis plays an important role in biomedical processes.⁵ ECs are vital functional cells associated with angiogenesis and are the target cells in most angiogenic-related studies.³⁴ The promotion of EC proliferation, migration and tube formation abilities of ECs is critical for angiogenesis. Many TCM formulas, herbal extracts, and compounds are thought to have “blood-activating” functions.³⁵ Some of the beneficial effects of these TCMs on the vascular system have been supported by modern medical theories. Treatments such as Danshen (*Salvia miltiorrhiza* Bunge.), Danggui (*Angelica sinensis*.), icariin (*Epimedium P.E.*) and Huangqi (*Astragalus membranaceus* Bunge.) extractions have been shown to exert outstanding angiogenic effects on ECs and accelerate wound healing or bone regeneration.^{29,36} Puerarin is the main



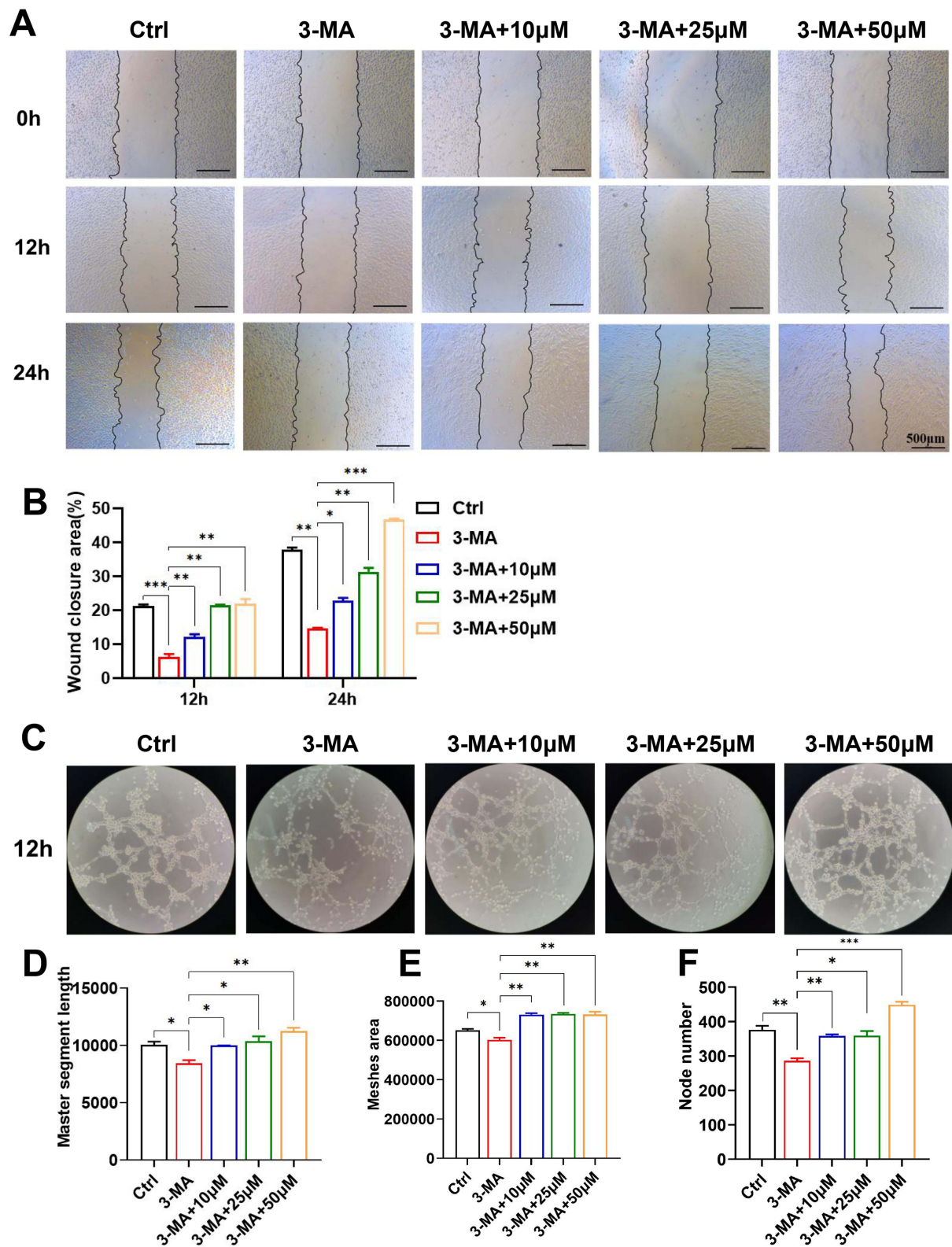


Figure 10 Puerarin alleviates the migration and tube formation dysfunction induced by autophagy inhibition. EA.hy926 cells were exposed to 3-MA + 10 µM, 3-MA + 25 and 3-MA + 50 µM puerarin. **(A and B)** Wound healing assays were performed to examine the cell migration ability (scale bars=500 µm). **(C–F)** Angiogenesis ability was confirmed by tube formation assays (Magnification: 100×). * $(P < 0.05)$, ** $(P < 0.01)$, *** $(P < 0.001)$.

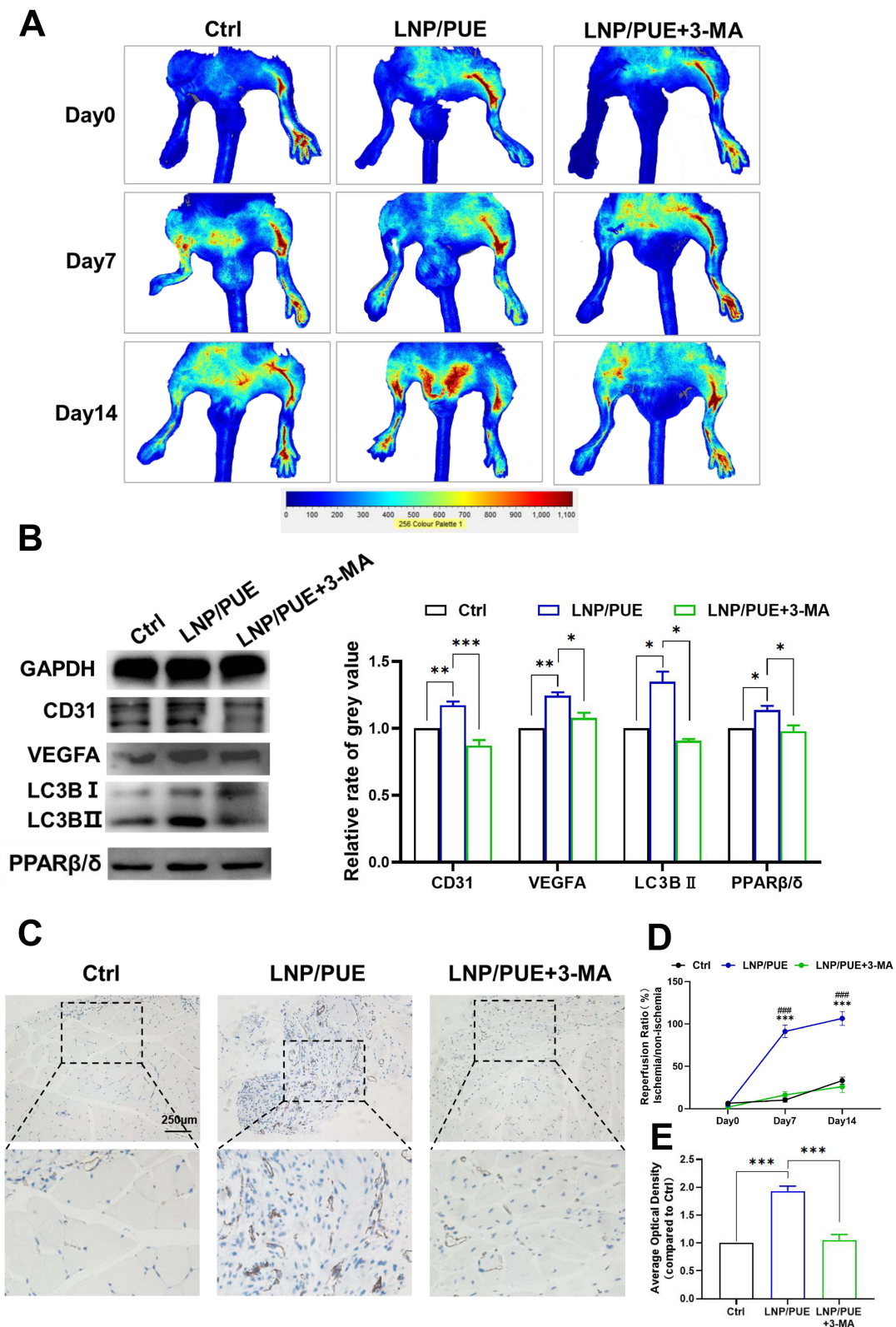


Figure 11 3-MA inhibited angiogenesis and autophagy activation mediated by the LNP/PUE-incorporated hydrogel. **(A)** Representative images of blood flow perfusion of hind-limb ischemia mice on day 0, 7 and 14 after the operation. **(B)** Western blot results and the statistical analysis of tissue samples. **(C)** CD31 immunohistochemical of gastrocnemius samples on day 14 after the operation (scale bars=250μm). **(D)** Statistical analysis of **(A)**. **(E)** Statistical of **(C)**. LNP/PUE(M) was used in the “LNP/PUE” groups, and 15 μL of 5 mg/mL 3-MA was used in the results in Figure 11. Compared with control: *($P < 0.05$), **($P < 0.01$), ***($P < 0.001$); compared with LNP/PUE + 3-MA: ####($P < 0.001$).

extract of *Puerariae Radix lobata*, one of the earliest crude herbs used in TCMs to treat diabetes, fever and other conditions.¹ Currently, puerarin is often used to treat the therapy of cardiovascular diseases such as hypertension and arrhythmia in China.^{37,38} The main molecular mechanisms underlying these therapeutic effects functions are anti-inflammatory, antioxidative stress and antiapoptotic effects.³⁹ For instance, puerarin can inhibit the inflammatory NF- κ B pathway,⁴⁰ oxidative stress-related MAPK pathway,⁴¹ apoptosis-related Bcl/Bax ratio,⁴² and PI3k/Akt pathway,⁴³ among other factors and pathways. In addition, puerarin can also act function as an open-channel blocker of IK1, which may explain the antiarrhythmic function of puerarin.⁴⁴ Although the beneficial effects of puerarin on the cardiovascular system have been well documented, its effect on vascular EC angiogenesis requires further examination. In this study, we prepared a puerarin sustained release system, demonstrated its angiogenic effect, and further explored the potential underlying mechanisms.

First, we demonstrated the angiogenic effect of puerarin in vivo in a mouse hind-limb ischemia model. The literature and our results both indicated that high concentrations of puerarin could induce toxicity; therefore, sustained administration of low doses was necessary. In previous studies of the therapeutic use of puerarin, multiple times of treatments were often required.⁴⁵⁻⁴⁷ To avoid excessive drug concentrations in the body, reduce the administration frequency and alleviate patient pain, the application of a sustained release system is necessary. Hydrogels have good biocompatibility and biodegradability, and are suitable for use as drug carriers in sustained release systems. The observation period of posterior limb ischemic healing is generally 7–14 days, but in our study, the release efficiency of GelMA/PUE was close to 100% within 7 days (Figure 1D), suggesting that the sustained release effect of GelMA/PUE alone did not last long enough. Similar results were also found in the study of Ou et al, in which the sustained release duration in the drug + hydrogel group was significantly shorter than that in the drug + carrier + hydrogel group. Therefore, to maintain therapeutic blood concentration, LNP was selected as scaffold to furtherly help the dispersion of PUE, and GelMA/LNP/PUE was prepared to achieve prolonged sustained release effect of puerarin. LNPs are novel, green biodegradable nanoparticles that have been proven to be effective in sustained release of a variety of TCMs.^{25,48} The FTIR results showed that the characteristic peaks of the prepared LNPs and the LNP/PUE were basically consistent, indicating that there were no chemical bonds formed after PUE was added.

Then, the LNP/PUE were blended into a hydrogel to prepare the GelMA/LNP/PUE sustained release system. According to the SEM results, the porous morphology and release efficiency of the prepared hydrogel were conducive to PUE dispersion and sustained release, respectively. Not only under pH=7.4 physiological environment, but also in pH=6.4 condition, PUE showed effective sustained release effects. A pH of 6.4 was selected because the pH value of acute and chronic wounds or necrotic tissues is acidic. In a study by Shi et al, pH 6.4 was used to simulate the angiogenic microenvironment of the wound area to explore the slow-release effect of drugs.⁴⁹

Next, we demonstrated the materials' therapeutic effect on mouse hind-limb ischemia. After each group of hydrogels was applied to the mouse hind-limb ischemia model, puerarin significantly alleviated blood flow on days 7 and 14 after surgery. Immunohistochemical staining of day 14 samples also showed that neovascularization in the LNP/PUE(M) and LNP/PUE(H) groups was prominently promoted. Similar results were observed by WB of animal tissue samples. The addition of puerarin significantly increased the vascular EC marker CD31 and angiogenesis indicator VEGFA. The prepared hydrogels we prepared, especially those in the medium concentration groups, had an evident proangiogenic effect. Moreover, compared with that in the control groups, there was no difference in angiogenesis in the LNP groups, suggesting that it was puerarin that played a major role in angiogenesis in response to the materials we constructed. In the study by Jin et al, puerarin-induced CD31 elevation and promoted angiogenesis were also detected in mice with transverse aorta constriction.⁵⁰ Zhang et al also reported VEGF enhancement in ischemic myocardium of puerarin-treated of rats.⁵¹ Our results are consistent with these existing studies, confirming the effectiveness of puerarin in angiogenesis in vivo, and the sustained-release system we constructed was also effective in mediating angiogenesis.

Therefore, in the following studies, we hope to further explore the mechanism of puerarin-promoted angiogenesis through in vitro experiments. EA.hy926 cells were used to construct an in vitro model. The effect of puerarin on cell proliferation was detected. Puerarin was diluted to 5, 10, 25, 50 and 100 μ M, and incubated with the cells for 6, 24 and 48 h. The results shown in Figure 3A suggest that all of the concentrations except for 5 μ M promoted cell viability starting at 6 h. At 24 h, 5 μ M puerarin also enhanced cell proliferation, but this effect was not maintained until 48 h. As

previously reported, the proliferation ability of ECs is also an essential function for neovascularization.⁵² The effect of 5 μM puerarin on promoting cell proliferation began later and was maintained for a short time; thus, we hypothesize that its effect is less significant than that observed in response to higher concentrations, and it would be difficult to achieve the expected effect and explore the underlying cytological mechanism of proangiogenic effect. Puerarin (100 μM) significantly induced cytotoxicity at 24 and 48 h. This dual effect of puerarin on cell viability indicates the importance of the concentration range in the therapeutic applications of puerarin. Because this work aimed to explore the therapeutic effects of puerarin, its biocompatibility is critical, and a concentration of 100 μM was therefore excluded. To further confirm the puerarin concentrations, we reviewed existing literature. In other current studies, the concentrations of puerarin that effectively protected ECs included 10, 25, 30, and 50 μM . Within this concentration range, puerarin has a significant effect on protecting the viability and promoting the cellular function of ECs,¹² which is consistent with our hypothesis. Therefore, 10, 25 and 50 μM puerarin were used in the following experiments.

Migration and tube formation are vital features of angiogenic capacity.³³ Therefore, to evaluate the effect of puerarin on the angiogenesis of EA.hy926 cells, wound healing and tube formation assays were performed. As shown in Figure 3B and C, 10, 25 and 50 μM puerarin prominently accelerated the wound recovery rate. However, difference was not observed among the three puerarin-treated groups at 12 h. At 24 h, the recovery area in the 50 μM groups was markedly larger than those of the control and 10 μM groups. This result was consistent with the study by Jin et al, who reported that 10, 25 and 50 μM puerarin could effectively promote HUVEC migration rate.⁵⁰ Similarly, our tube formation assay also indicated that puerarin induced a longer master segment length and larger node junction numbers and meshes area than the control values. We further confirmed the proangiogenic effect of puerarin at the mRNA and protein levels. The VEGF pathway and ANG/Tie axis are two vital signal transduction pathways involved in angiogenesis and are considered classic indicators.^{53,54} VEGF is the most specific growth factor that is active during angiogenesis: VEGF is involved in migration and proliferation and induces the permeabilization of vessels; VEGFR2 is the specific receptor of VEGF, and an increase in the levels of this receptor indicates the promotion of angiogenesis.^{53,55} ANG1 and ANG2 are competitively antagonistic, and can activate the Tie2 receptor and promote EC migration and vessel stabilization. ANG1 has been shown to be highly expressed in the tumor vasculature, and changes in its expression level can reflect the changes in angiogenesis; ANG2 can also bind to Tie2 to regulate angiogenesis.^{55,56} Therefore, we subsequently determined the levels of VEGFA, VEGFR2, ANG1, ANG2 and Tie2 by qPCR and WB. The qPCR results showed increases in VEGF and VEGFR2 levels, but the changes in ANG, ANG2 and Tie2 were not significant. It has been suggested by a recent study that puerarin could promote the expression of ANG1 and ANG2 in rats with myocardial infarction.⁸ However, our results indicated that the levels of ANG1 and ANG2 did not differ from those of the control. This effect may be due to differences in experimental models and differences between *in vivo* and *in vitro* experiments. Then, the protein expression of VEGFA and VEGFR2 in puerarin-treated cells was measured. The results indicated the upregulation of these two angiogenic indicators. These changes in these of proangiogenic molecule levels are consistent with our morphological results and confirm that puerarin can effectively promote angiogenesis in ECs.

Autophagy, which promotes the recycling of intracellular substances, is a necessary process for the maintenance of normal cellular activities.^{10,57} Regulating autophagy levels has become a prominent therapeutic strategy for many diseases.⁵⁸ Enhanced autophagy in vessels is considered a necessary process associated with the dynamic adaptation of ECs to bioenergetic needs during angiogenesis.⁵⁹ Many herbal TCMs have been shown to be effective in treating cardiovascular diseases, nervous system diseases and diabetes due to their regulation of autophagy.^{60–62} Studies have indicated that puerarin can also affect autophagy levels in different types of cell lines or tissues. In kidney podocytes, puerarin induces autophagosome production, increases LC3II expression and decreases p62 levels, which attenuates diabetic nephropathy.⁶³ An *in vivo* study suggested that puerarin could restore autophagy through activation of the AMPK/mTOR pathway in rats and thereby protect against cardiomyocyte hypertrophy.⁶⁴ In contrast, puerarin-mediated autophagy inhibition has also been reported. Autophagy suppression was observed in puerarin-treated osteoclast precursors, and osteoclast precursor proliferation and osteoclast differentiation were blocked.⁶⁵ Another study indicated that puerarin decreased LC3II levels and p62 degradation and helped to relieve myocardial ischemia/reperfusion injury, and this autophagy suppression might be caused by a puerarin-induced Akt increase.⁶⁶ These findings suggest that puerarin can affect autophagy. Notably, the contradictory regulatory effects might be due to the differences in drug

concentrations and experimental models in these researches. Our MTT results above also indicated similar bidirectional regulation; although 10, 25 and 50 μM puerarin could promote EA.hy926 cell proliferation, cell viability was suppressed by prolonged exposure to higher concentrations of puerarin. Subsequently, we examined how puerarin regulates autophagy in EA.hy926 cells and whether it further affects angiogenesis. LC3II is a recognized indicator of autophagy. During autophagy process, LC3I in the cytoplasm is enzymatically converted into membrane-bound LC3II, which is located on the autophagosome membrane.⁶⁷ As shown in Figure 6, the LC3II levels were increased in all three puerarin-treated groups, which suggested that autophagosome formation was promoted. p62 is a key autophagy receptor that can connect cargo and autophagosomes and then enter autophagic lysosomes to complete the degradation of ubiquitinated substrates.⁶⁸ In the 10 μM puerarin-treated group, p62 downregulation was observed at 3, 6, 12 and 24 h, and in the 25 μM group, this decrease was observed at 1 h, which suggested that autophagic degradation was mediated by puerarin in EA.hy926 cells. It is worth noting that in the 50 μM puerarin-treated groups, the p62 expression levels were increased at 1 and 3 h and then decreased gradually to levels lower than those in the control group at 12 and 24 h. Although the increased p62 levels is generally considered a marker of autophagy inhibition, during the analysis, it is not uncommon to see that autophagy activation is not uncommonly accompanied by the upregulation of p62 expression.^{32,69} One potential reason may be that p62, which is a stress protein, is greatly increased in response to sudden changes in the cellular environment.⁷⁰ In response to a high concentration of puerarin, excessive autophagosome formation of is observed during the early stage, and these autophagosomes cannot be degraded by autophagic lysosomes in a timely manner. Therefore, temporary p62 accumulation is observed, indicating a “pseudo” autophagy blockade. This finding may help to explain why 100 μM puerarin inhibited cell activity. This effect might be due to the overproduction of autophagosomes, which far exceeds the degradation capacity of autophagolysosomes, and their excessive accumulation results in subsequent adverse effects, thereby leading to the suppression of proliferation. This finding also reminds us to strictly control the selection of puerarin concentration when studying the biomedical applications of puerarin. Overall, these results demonstrate that puerarin activates autophagy, and in subsequent experiments, we explored the effects of puerarin-induced autophagy on angiogenesis.

Consistent with current reports, our results indicate that 3-MA exposure can inhibit the expression of the angiogenic factors VEGFA and VEGFR2, EC migration and tube formation. Moreover, the use of puerarin clearly alleviated the reduction in the angiogenic ability of ECs. These results are consistent with our *in vivo* evidence, which demonstrated that 3-MA can significantly inhibit the puerarin-mediated upregulation of VEGFA and CD31 in mouse tissue. This evidence strongly suggests that autophagy is a key intermediate step in puerarin-mediated angiogenesis. Autophagy in ECs is closely associated with metabolic pathways and lipid homeostasis.⁹ PPARs belong to the superfamily of ligand-activated transcription factors, and they play key roles in lipid metabolism, adipogenesis, insulin sensitivity and blood pressure regulation.⁷¹ The PPAR family member PPAR β/δ is considered an angiogenesis promoter. It has been reported that there is a PPAR response element on the VEGFA promoter, which might explain the PPAR β/δ activation-induced VEGFA mRNA expression and the subsequent promotion of angiogenesis.⁷² An increase in MMP-9 mRNA level was also observed in ECs after exposure to a PPAR β/δ agonist. MMP-9 is involved in proteolysis and remodeling of the extracellular matrix,⁷³ and its upregulation can aid EC migration. Other angiogenesis pathways, such as the PDGF/PDGFR pathway and c-Kit, can also be triggered by PPAR β/δ activation.⁷⁴ Moreover, PPAR β/δ has a close relationship with cellular fatty acid metabolism and antiapoptotic effects, which might also be beneficial in EC proliferation and other cellular functions of ECs needed for angiogenesis.^{18,75} However, in the literature, whether puerarin-mediated autophagy can regulate PPAR β/δ is unclear, although it can promote the elevation of the PPAR family homologs, PPAR- α ⁷⁶ and PPAR- γ .⁷⁷ Here in our *in vivo* study, PPAR β/δ was increased in the LNP/PUE(M) and LNP/PUE(H) groups *in vivo*. *In vitro* experiments showed that PPAR β/δ levels in the 10, 25 and 50 μM puerarin groups were also significantly increased. Exposure to the autophagy inhibitor 3-MA downregulated PPAR β/δ expression *in vivo* and *in vitro*, but the level was restored by puerarin, which indicated that puerarin could regulate PPAR β/δ levels by promoting autophagy. Notably, another existing study suggested that PPAR β/δ was an upstream regulator of autophagy, that could trigger AMPK/mTOR pathway-mediated autophagy in BMSCs and thus accelerate bone regeneration.¹⁹ Whether this downstream/upstream difference is due to there is indeed feedback loop regulation between autophagy and PPAR β/δ or caused by experimental conditions is unclear, and we will further explore the role of PPAR β/δ and autophagy in angiogenesis in future studies.

Conclusion

The LNP/PUE-incorporated hydrogel was prepared and characterized. We demonstrated the angiogenic effect of puerarin on mouse hind-limb ischemia and EA.hy926 cells and explored the potential underlying mechanisms. Our findings suggest that puerarin can promote autophagy, induce the expression of the angiogenic factor PPAR β/δ , and thereby mediate angiogenesis in EA.hy926 cells. The findings will hopefully be helpful in studying the angiogenic applications of puerarin and will provide a theoretical basis for the therapeutic effect of puerarin on the cardiovascular system.

Abbreviations

TCM, traditional Chinese medicine; EC, endothelial cell; EMT, endothelial-mesenchymal transition; PPAR, peroxisome proliferator-activated receptor; LNPs, lignin nanoparticles; LNP/PUE, puerarin-attached lignin nanoparticles; DMEM, Dulbecco's modified Eagle's medium; FBS, fetal bovine serum; 3-MA, 3-methyladenine; DMSO, dimethyl sulfoxide; WB, Western blotting; qPCR, quantitative real-time polymerase chain reaction; WB, Western blot.

Acknowledgments

Yingjing Pan and Tianci Lin are co-first authors for this study. This work was supported by the Scientific Research Project of the Traditional Chinese Medicine Bureau of Guangdong Province under Grant 20212156 and 20192061; the Guangdong Basic and Applied Basic Research Foundation under Grant 2019A1515110088; the Medical Scientific Research Foundation of Guangdong Province under Grant A2020227; and the International Science and Technology Cooperation Project of Science and Technological Bureau of Guangzhou Huangpu District under Grant 2019GH11 and 2020GH14.

Disclosure

The authors report no conflicts of interest in this work.

References

1. Zhou Y, Zhang H, Peng C. Puerarin: a review of pharmacological effects. *Phytother Res*. 2014;28(7):961–975. doi:10.1002/ptr.5083
2. Zhang L, Liu L, Wang M. Effects of puerarin on chronic inflammation: focus on the heart, brain, and arteries. *Aging Med*. 2021;4(4):317–324. doi:10.1002/agm2.12189
3. Liu B, Tan Y, Wang D, Liu M. Puerarin for ischaemic stroke. *Cochrane Database Syst Rev*. 2016;2:CD004955. doi:10.1002/14651858.CD004955.pub3
4. Wu X, Rebol MR, Korf-Klingebiel M, Wollert KC. Angiogenesis after acute myocardial infarction. *Cardiovasc Res*. 2021;117(5):1257–1273. doi:10.1093/cvr/cvaa287
5. Reddy LVK, Murugan D, Mullick M, Begum Moghal ET, Sen D. Recent approaches for angiogenesis in search of successful tissue engineering and regeneration. *Curr Stem Cell Res Ther*. 2020;15(2):111–134. doi:10.2174/1574888X14666191104151928
6. Chang XZT, Liu D, Meng Q, et al. Puerarin attenuates LPS-induced inflammatory responses and oxidative stress injury in human umbilical vein endothelial cells through mitochondrial quality control. *Oxid Med Cell Longev*. 2021;2021:6659240. doi:10.1155/2021/6659240
7. Li X, Chen D, Yuan T, et al. Puerarin attenuates the endothelial-mesenchymal transition induced by oxidative stress in human coronary artery endothelial cells through PI3K/AKT pathway. *Eur J Pharmacol*. 2020;886:173472. doi:10.1016/j.ejphar.2020.173472
8. Guo BQ, Xu JB, Xiao M, Ding M, Duan LJ. Puerarin reduces ischemia/reperfusion-induced myocardial injury in diabetic rats via upregulation of vascular endothelial growth factor A/angiotensin-1 and suppression of apoptosis. *Mol Med Rep*. 2018;17(5):7421–7427. doi:10.3892/mmr.2018.8754
9. Schaaf MB, Houbaert D, Meçe O, Agostinis P. Autophagy in endothelial cells and tumor angiogenesis. *Cell Death Differ*. 2019;26(4):665–679. doi:10.1038/s41418-019-0287-8
10. Glick D, Barth S, Macleod KF. Autophagy: cellular and molecular mechanisms. *J Pathol*. 2010;221(1):3–12. doi:10.1002/path.2697
11. Zhu XR, Du JH. Autophagy: a potential target for the treatment of intraocular neovascularization. *Int J Ophthalmol*. 2018;11(4):695–698. doi:10.18240/ijo.2018.04.26
12. Adornetto A, Gesualdo C, Laganà ML, Trotta MC, Rossi S, Russo R. Autophagy: a novel pharmacological target in diabetic retinopathy. *Front Pharmacol*. 2021;12:695267. doi:10.3389/fphar.2021.695267
13. Zhang ZY, Bao XL, Cong YY, Fan B, Li GY. Autophagy in age-related macular degeneration: a regulatory mechanism of oxidative stress. *Oxid Med Cell Longev*. 2020;2020:2896036. doi:10.1155/2020/2896036
14. Jiang F. Autophagy in vascular endothelial cells. *Clin Exp Pharmacol Physiol*. 2016;43(11):1021–1028. doi:10.1111/1440-1681.12649
15. Li G, Rao H, Xu W. Puerarin plays a protective role in chondrocytes by activating Beclin1-dependent autophagy. *Biosci Biotechnol Biochem*. 2021;85(3):621–625. doi:10.1093/bbb/zbba078
16. Lian D, Yuan H, Yin X, et al. Puerarin inhibits hyperglycemia-induced inter-endothelial junction through suppressing endothelial Nlrp3 inflammasome activation via ROS-dependent oxidative pathway. *Phytomedicine*. 2019;55:310–319. doi:10.1016/j.phymed.2018.10.013

17. Hong F, Pan S, Guo Y, Xu P, Zhai Y. PPARs as nuclear receptors for nutrient and energy metabolism. *Molecules*. 2019;24(14):2545. doi:10.3390/molecules24142545
18. Schmidt A, Endo N, Rutledge SJ, Vogel R, Shinar D, Rodan GA. Identification of a new member of the steroid hormone receptor superfamily that is activated by a peroxisome proliferator and fatty acids. *Mol Endocrinol*. 1992;6(10):1634–1641. doi:10.1210/mend.6.10.1333051
19. Chen M, Jing D, Ye R, Yi J, Zhao Z. PPAR β/δ accelerates bone regeneration in diabetic mellitus by enhancing AMPK/mTOR pathway-mediated autophagy. *Stem Cell Res Ther*. 2021;12(1):566. doi:10.1186/s13287-021-02628-8
20. Tong L, Wang L, Yao S, et al. PPAR δ attenuates hepatic steatosis through autophagy-mediated fatty acid oxidation. *Cell Death Dis*. 2019;10(3):197. doi:10.1038/s41419-019-1458-8
21. Bishop-Bailey D. PPARs and angiogenesis. *Biochem Soc Trans*. 2011;39(6):1601–1605. doi:10.1042/BST20110643
22. Nanayakkara GK, Wyble J, Quindry J, Amin RH. Protective mechanism of PPAR-delta-HIF1 signaling in the ischemic diabetic heart. *FASEB Journal*. 2012;26(12):1363–1367.
23. Meissner M, Hrgovic I, Doll M, et al. Peroxisome proliferator-activated receptor {delta} activators induce IL-8 expression in nonstimulated endothelial cells in a transcriptional and posttranscriptional manner. *J Biol Chem*. 2010;285(44):33797–33804. doi:10.1074/jbc.M110.137943
24. Zuo X, Xu W, Xu M, et al. Metastasis regulation by PPAR δ expression in cancer cells. *JCI Insight*. 2017;2(1):e91419. doi:10.1172/jci.insight.91419
25. Schneider WDH, Dillon A, Camassola M. Lignin nanoparticles enter the scene: a promising versatile green tool for multiple applications. *Biotechnol Adv*. 2021;47:107685. doi:10.1016/j.biotechadv.2020.107685
26. Ou Q, Zhang S, Fu C, et al. More natural more better: triple natural anti-oxidant puerarin/ferulic acid/polydopamine incorporated hydrogel for wound healing. *J Nanobiotechnology*. 2021;19(1):237. doi:10.1186/s12951-021-00973-7
27. Padgett ME, McCord TJ, McClung JM, Kontos CD. Methods for Acute and Subacute Murine Hindlimb Ischemia. *J Vis Exp*. 2016;112:54166.
28. Zhou X, Razmovski-Naumovski V, Kam A, et al. Synergistic study of a Danshen (*Salvia Miltiorrhizae Radix et Rhizoma*) and Sanqi (*Notoginseng Radix et Rhizoma*) combination on cell survival in EA.hy926 cells. *BMC Complement Altern Med*. 2019;19(1):50. doi:10.1186/s12906-019-2458-z
29. Li X, Wen Y, Sheng L, Guo R, Zhang Y, Shao L. Icaritin activates autophagy to trigger TGF β 1 upregulation and promote angiogenesis in EA.hy926 human vascular endothelial cells. *Bioengineered*. 2022;13(1):164–177. doi:10.1080/21655979.2021.2011637
30. Mishra A, Behura A, Kumar A, et al. Soybean lectin induces autophagy through P2RX7 dependent activation of NF- κ B-ROS pathway to kill intracellular mycobacteria. *Biochim Biophys Acta Gen Subj*. 2021;1865(2):129806. doi:10.1016/j.bbagen.2020.129806
31. Carpentier G, Berndt S, Ferratge S, et al. Angiogenesis analyzer for ImageJ - A comparative morphometric analysis of “Endothelial Tube Formation Assay” and “Fibrin Bead Assay”. *Sci Rep*. 2020;10(1):14. doi:10.1038/s41598-020-67289-8
32. Xu A, Yang Y, Shao Y, Wu M, Sun Y. Activation of cannabinoid receptor type 2-induced osteogenic differentiation involves autophagy induction and p62-mediated Nrf2 deactivation. *Cell Commun Signal*. 2020;18(1):9. doi:10.1186/s12964-020-0512-6
33. Nowak-Sliwinska P, Alitalo K, Allen E, et al. Consensus guidelines for the use and interpretation of angiogenesis assays. *Angiogenesis*. 2018;21(3):425–532. doi:10.1007/s10456-018-9613-x
34. Krüger-Genge A, Bloki A, Franke RP, Jung F. Vascular endothelial cell biology: an update. *Int J Mol Sci*. 2019;20(18):4411. doi:10.3390/ijms20184411
35. Tao L, Wang S, Zhao Y, et al. Pleiotropic effects of herbs characterized with blood-activating and stasis-resolving functions on angiogenesis. *Chin J Integr Med*. 2016;22(10):795–800. doi:10.1007/s11655-015-2405-x
36. Bu L, Dai O, Zhou F, et al. Traditional Chinese medicine formulas, extracts, and compounds promote angiogenesis. *Biomed Pharmacother*. 2020;132:110855. doi:10.1016/j.biopha.2020.110855
37. Xie B, Wang Q, Zhou C, Wu J, Xu D. Efficacy and safety of the injection of the Traditional Chinese Medicine Puerarin for the treatment of diabetic peripheral neuropathy: a systematic review and meta-analysis of 53 randomized controlled trials. *Evid Based Complement Alternat Med*. 2018;2018:2834650. doi:10.1155/2018/2834650
38. F X. Effect of puerarin injection combined with amiodarone on cardiac arrhythmia after PCI. *J Clin Ration Drug Use*. 2020;13(16):12–13 + 16.
39. Zhou YX, Zhang H, Peng C. Effects of puerarin on the prevention and treatment of cardiovascular diseases. *Front Pharmacol*. 2021;12:771793. doi:10.3389/fphar.2021.771793
40. Liu Q, Wang C, Meng Q, et al. Puerarin sensitized K562/ADR cells by inhibiting NF- κ B pathway and inducing autophagy. *Phytother Res*. 2021;35(3):1658–1668. doi:10.1002/ptr.6932
41. Zeng XP, Zeng J, Lin X, et al. Puerarin ameliorates caerulein-induced chronic pancreatitis via inhibition of MAPK signaling pathway. *Front Pharmacol*. 2021;12:686992. doi:10.3389/fphar.2021.686992
42. Wang N, Zhang Y, Wu L, et al. Puerarin protected the brain from cerebral ischemia injury via astrocyte apoptosis inhibition. *Neuropharmacology*. 2014;79:282–289. doi:10.1016/j.neuropharm.2013.12.004
43. Zhao GJ, Hou N, Cai SA, et al. Contributions of Nrf2 to puerarin prevention of cardiac hypertrophy and its metabolic enzymes expression in rats. *J Pharmacol Exp Ther*. 2018;366(3):458–469. doi:10.1124/jpet.118.248369
44. Zhang H, Zhang L, Zhang Q, et al. Puerarin: a novel antagonist to inward rectifier potassium channel (IK1). *Mol Cell Biochem*. 2011;352(1–2):117–123. doi:10.1007/s11010-011-0746-0
45. Zhao J, Luo D, Liang Z, Lao L, Rong J. Plant natural product puerarin ameliorates depressive behaviors and chronic pain in mice with Spared Nerve Injury (SNI). *Mol Neurobiol*. 2017;54(4):2801–2812. doi:10.1007/s12035-016-9870-x
46. Peng Y, Wang L, Zhao X, et al. Puerarin attenuates lipopolysaccharide-induced myocardial injury via the 14-3-3 γ /PKC ϵ pathway activating adaptive autophagy. *Int Immunopharmacol*. 2022;108:108905. doi:10.1016/j.intimp.2022.108905
47. Niu P, Sun Y, Wang S, et al. Puerarin alleviates the ototoxicity of gentamicin by inhibiting the mitochondria-dependent apoptosis pathway. *Mol Med Rep*. 2021;24(6):851. doi:10.3892/mmr.2021.12491
48. Da L, Liu R, Hu LQ, Zou Z, Si C. Lignin nanoparticle as a novel green carrier for the efficient delivery of resveratrol. *ACS Sustain Chem Eng*. 2017;5(9):8241–8249. doi:10.1021/acssuschemeng.7b01903
49. Shi M, Zhang H, Song T, et al. Sustainable dual release of antibiotic and growth factor from pH-responsive uniform alginate composite microparticles to enhance wound healing. *ACS Appl Mater Interfaces*. 2019;11(25):22730–22744. doi:10.1021/acsami.9b04750
50. Jin YG, Yuan Y, Wu QQ, et al. Puerarin protects against cardiac fibrosis associated with the inhibition of TGF- β 1/Smad2-mediated endothelial-to-mesenchymal transition. *PPAR Res*. 2017;2017:2647129. doi:10.1155/2017/2647129

51. Zhang S, Chen S, Shen Y, et al. Puerarin induces angiogenesis in myocardium of rat with myocardial infarction. *Biol Pharm Bull.* 2006;29(5):945–950. doi:10.1248/bpb.29.945
52. Benson CE, Southgate L. The DOCK protein family in vascular development and disease. *Angiogenesis.* 2021;24(3):417–433. doi:10.1007/s10456-021-09768-8
53. Melincovici CS, Boşca A, Şuşman S, et al. Vascular endothelial growth factor (VEGF) - key factor in normal and pathological angiogenesis. *Rom J Morphol Embryol.* 2018;59(2):455–467.
54. Eklund L, Kangas J, Saharinen P. Angiopoietin-Tie signalling in the cardiovascular and lymphatic systems. *Clin Sci.* 2017;131(1):87–103. doi:10.1042/CS20160129
55. Akwii RG, Sajib MS, Zahra FT, Mikelis CM. Role of angiopoietin-2 in vascular physiology and pathophysiology. *Cells.* 2019;8(5):471. doi:10.3390/cells8050471
56. Fagiani E, Christofori G. Angiopoietins in angiogenesis. *Cancer Lett.* 2013;328(1):18–26. doi:10.1016/j.canlet.2012.08.018
57. Ajoalabady A, Aghanejad A, Bi Y, et al. Enzyme-based autophagy in anti-neoplastic management: from molecular mechanisms to clinical therapeutics. *Biochim Biophys Acta Rev Cancer.* 2020;1874(1):188366. doi:10.1016/j.bbcan.2020.188366
58. Jiang G, Tan Y, Wang H, et al. The relationship between autophagy and the immune system and its applications for tumor immunotherapy. *Mol Cancer.* 2019;18(1):17. doi:10.1186/s12943-019-0944-z
59. Mamei E, Martello A, Caporali A. Autophagy at the interface of endothelial cell homeostasis and vascular disease. *FEBS J.* 2021;289(11):2976–2991. doi:10.1111/febs.15873
60. Xin GJ, Fu JH, Li L, et al. Research progress of traditional Chinese medicine in regulating autophagy and ischemic heart disease. *Zhongguo Zhong Yao Za Zhi.* 2020;45(16):3784–3789. doi:10.19540/j.cnki.cjcm.20200113.401
61. Wang ZY, Liu J, Zhu Z, et al. Traditional Chinese medicine compounds regulate autophagy for treating neurodegenerative disease: a mechanism review. *Biomed Pharmacother.* 2021;133:110968. doi:10.1016/j.biopha.2020.110968
62. Wang Y, Zhao H, Wang Q, et al. Chinese Herbal Medicine in ameliorating diabetic kidney disease via activating autophagy. *J Diabetes Res.* 2019;2019:9030893. doi:10.1155/2019/9030893
63. Li X, Zhu Q, Zheng R, et al. Puerarin attenuates diabetic nephropathy by promoting autophagy in podocytes. *Front Physiol.* 2020;11:73. doi:10.3389/fphys.2020.00073
64. Song X, Li Z, Liu F, Wang Z, Wang L. Restoration of autophagy by puerarin in lead-exposed primary rat proximal tubular cells via regulating AMPK-mTOR signaling. *J Biochem Mol Toxicol.* 2017;31(3):e21869. doi:10.1002/jbt.21869
65. Zhang GWY, Tang G, Ma Y, Ma Y. Puerarin inhibits the osteoclastogenesis by inhibiting RANKL-dependent and -independent autophagic responses. *BMC Complement Altern Med.* 2019;19(1):269. doi:10.1186/s12906-019-2691-5
66. Wang JF, Mei ZG, Fu Y, et al. Puerarin protects rat brain against ischemia/reperfusion injury by suppressing autophagy via the AMPK-mTOR-ULK1 signaling pathway. *Neural Regen Res.* 2018;13(6):989–998. doi:10.4103/1673-5374.233441
67. Shaid S, Brandts C, Serve H, Dikic I. Ubiquitination and selective autophagy. *Cell Death Differ.* 2013;20(1):21–30. doi:10.1038/cdd.2012.72
68. Lamark TSS, Johansen T, Johansen T. Regulation of selective autophagy: the p62/SQSTM1 paradigm. *Essays Biochem.* 2017;61(6):609–624. doi:10.1042/EBC20170035
69. Li RF, Chen G, Ren JG, et al. The adaptor protein p62 is involved in RANKL-induced autophagy and osteoclastogenesis. *J Histochem Cytochem.* 2014;62(12):879–888. doi:10.1369/0022155414551367
70. Katsuragi Y, Ichimura Y, Komatsu M. p62/SQSTM1 functions as a signaling hub and an autophagy adaptor. *FEBS J.* 2015;282(24):4672–4678. doi:10.1111/febs.13540
71. Wagner N, Wagner K. The role of PPARs in disease. *Cells.* 2020;9(11):2367. doi:10.3390/cells9112367
72. Piqueras L, Reynolds AR, Hovalva-Dilke KM, et al. Activation of PPARbeta/delta induces endothelial cell proliferation and angiogenesis. *Arterioscler Thromb Vasc Biol.* 2007;27(1):63–69. doi:10.1161/01.ATV.0000250972.83623.61
73. Kanayasu-Toyoda T, Tanake T, Ishii-Watabe A, et al. Angiogenic role of MMP-2/9 expressed on the cell surface of early endothelial progenitor cells/myeloid angiogenic cells. *J Cell Physiol.* 2015;230(11):2763–2775. doi:10.1002/jcp.25002
74. Wagner N, Wagner K. PPARs and angiogenesis-implications in pathology. *Int J Mol Sci.* 2020;21(16):5723. doi:10.3390/ijms21165723
75. Liou JY, Lee S, Ghelani D, Matijevec-Aleksic N, Wu KK. Protection of endothelial survival by peroxisome proliferator-activated receptor-delta mediated 14-3-3 upregulation. *Arterioscler Thromb Vasc Biol.* 2006;26(7):1481–1487. doi:10.1161/01.ATV.0000223875.14120.93
76. Hou N, Huang Y, Cai S, et al. Puerarin ameliorated pressure overload-induced cardiac hypertrophy in ovariectomized rats through activation of the PPARα/PGC-1 pathway. *Acta Pharmacol Sin.* 2021;42(1):55–67. doi:10.1038/s41401-020-0401-y
77. Yun J, Yu Y, Zhou G, et al. Effects of puerarin on the AKT signaling pathway in bovine preadipocyte differentiation. *Asian Austr J Anim Sci.* 2020;33(1):4–11. doi:10.5713/ajas.19.0004